Davies, P. J., McKenzie, J. A., Palmer-Julson, A., et al., 1991
*Proceedings of the Ocean Drilling Program, Initial Reports,* Vol. 133

# 6. SITE 813[1]

Shipboard Scientific Party[2]

## HOLE 813A

**Date occupied:** 24 August 1990

**Date departed:** 24 August 1990

**Time on hole:** 17 hr, 10 min

**Position:** 17°49.959′S, 149°29.669′E

**Bottom felt (rig floor; m, drill-pipe measurement):** 550.2

**Distance between rig floor and sea level (m):** 11.08

**Water depth (drill-pipe measurement from sea level, m):** 539.1

**Total depth (rig floor; m):** 781.7

**Penetration (m):** 231.5

**Number of cores (including cores with no recovery):** 26

**Total length of cored section (m):** 231.6

**Total core recovered (m):** 199.43

**Core recovery (%):** 86.1

**Oldest sediment recovered:**
Depth (mbsf): 231.5
Nature: microcrystalline dolomite
Age: middle Miocene or older

## HOLE 813B

**Date occupied:** 24 August 1990

**Date departed:** 25 August 1990

**Time on hole:** 13 hr, 34 min

**Position:** 17°49.951′S, 149°29.673′E

**Bottom felt (rig floor; m, drill-pipe measurement):** 549.9

**Distance between rig floor and sea level (m):** 11.08

**Water depth (drill-pipe measurement from sea level, m):** 538.9

**Total depth (rig floor, m):** 739.9

**Penetration (m):** 190.0

**Number of cores (including cores with no recovery):** 21

**Total length of cored section (m):** 190.0

**Total core recovered (m):** 196.19

**Core recovery (%):** 103.2

**Oldest sediment recovered:**
Depth (mbsf): 190.0
Nature: foraminifer micrite chalk
Age: middle Miocene

**Principal results:** Site 813 (proposed site NEA-10A/3) together with Sites 812 and 814 are located on the southwestern edge of the extensive Tregrosse/Lihou/Coringa Bank complex. This three-site transect was intended to study facies distribution in response to sea-level change across a platform-slope transition in a pure carbonate system. Site 813 represents the most distal part of an aggradational/progradational sequence.

Double-APC coring penetrated a 231.5-m-thick sequence of drowned platform sediments (average $CaCO_3$ = >95%) ranging in age from middle Miocene to Pleistocene. Benthic foraminiferal assemblages indicate a progressively increasing water depth from a shallow neritic setting (0–100 m) in the middle Miocene to an upper bathyal environment (200–600 m) during the Pliocene and Pleistocene.

Five major sedimentary units were recovered between the seafloor and 231.5 mbsf (meters below sea floor). Lithologic units are as follows:

1. Unit I: depth, 0–76.8 mbsf; age, Pleistocene to Pliocene. The sediments are essentially homogenous, micritic, foraminiferal to foraminiferal nannofossil ooze with bioclasts. The generally high nannofossil content (50%–80%) is consistent with a predominantly pelagic origin for the ooze, but variable degrees of induration throughout the interval suggest that the flux of metastable bank-derived carbonates—having a greater diagenetic potential—was not constant. Benthic foraminifers indicate an upper bathyal paleowater depth (200–600 m).
2. Unit II: depth, 76.8–117 mbsf; age, Pliocene–late Miocene. This unit consists of nannofossil foraminiferal ooze with micrite. The upper boundary is marked by salmon-colored, granular foraminiferal ooze containing reddish brown to reddish yellow, presumably iron-stained particles mixed with *in situ* foraminifers, bioclasts, and grains of indeterminate origin. In the lower part of the unit, the ooze is characterized by the presence of dark grains that are phosphatized benthic foraminifers. Benthic foraminiferal assemblages indicate that deposition of Unit II occurred during the transition from an outer neritic to uppermost bathyal paleobathymetric setting (100–300 m).
3. Unit III: depth, 117–160 mbsf; age, late Miocene. Bioclastic foraminiferal ooze with micrite and nannofossils; this unit differs from the overlying units in having a reduced nannofossil content (~20%–30%) in the fine fraction relative to the overlying oozes (which contain 50%–80% nannofossils). This difference suggests that there was a larger input of bank-derived metastable carbonate during this period. Such sediments are designated as periplatform oozes.
4. Unit IV: depth, 160 to ~195 mbsf; age, late Miocene–middle Miocene. Sediments of this unit are dolomitized, semi-lithified to lithified foraminiferal micritic chalks containing bioclasts interbedded with dolomitized, unlithified to semi-lithified micritic foraminiferal ooze containing bioclasts and nannofossils. The basal 3 m contains dolomitized, bioclastic nannofossil chalk interbedded with dolomitic foraminiferal rudstone and packstone. The larger benthic foraminifers indicate that deposition occurred in the middle to outer neritic zone (50–200 m).
5. Unit V: depth, ~195–231 mbsf; age, middle Miocene or older(?). Extremely poor recovery in this interval yielded only fragments of completely dolomitized skeletal grainstones and microcrystalline dolomite. Dolomitization is largely fabric destructive, but we nevertheless recognized such skeletal elements as calcareous algae and foraminifers. These biota suggest a shallow neritic environment (10–50 m) adjacent to or on the carbonate bank.

The sedimentation rate for the upper Pliocene to Pleistocene interval was 2.2 cm/k.y., succeeding a rate of about 1.2 cm/k.y. during the early Pliocene. During the latest late Miocene, the

[1] Davies, P. J., McKenzie, J. A., Palmer-Julson, A., et al., 1991. *Proc. ODP, Init. Repts.*, 133: College Station, TX (Ocean Drilling Program).
[2] Shipboard Scientific Party is as given in list of participants preceding the contents.

sedimentation rate was 3 cm/k.y. Nannofossil foraminiferal oozes of lithologic Unit II were deposited during the earliest late Pliocene to late Miocene and are distinguished from the overlying and underlying oozes by the inclusion of numerous iron-stained and/or phosphatized particles. In addition, a major change in physical properties (e.g., lower velocity and increased porosity and water content) occurs between 64.2 and 102.4 mbsf, generally encompassing most of Unit II. These properties suggest that the fine particles in the ooze may have been winnowed away, leaving behind a coarser grained, more porous sediment. The concentration of iron-stained and phosphatized reworked particles in the oozes requires a source area wherein these chemical alterations occurred, possibly associated with the contemporaneous condensed sequence recovered at nearby Site 814.

X-ray diffractograms of selected samples detected the presence of authigenic dolomite, which increases in abundance with depth from 1.3% at 2.3 mbsf to 78.2% at 193.7 mbsf. Unit V contains 100% microcrystalline dolomite. Aragonite concentrations up to 32% were recorded at 2.3 mbsf and progressively decreased with depth, being absent below 22.7 mbsf. A slight increase above seawater values in $Sr^{+2}$ and $Ca^{+2}$ concentrations between 0 and 22.7 mbsf suggests dissolution of metastable carbonate phases. Below this dissolution level, the $Sr^{+2}$, $Ca^{+2}$, and $Mg^{+2}$ concentrations remain constant with depth to between 89.2 and 107.5 mbsf, where distinct shifts in the $Sr^{+2}$, $Ca^{+2}$, and $Mg^{+2}$ concentrations occur. Below 107.5 mbsf, deeper values are constant to the base of the sampled section. The interstitial water chemistry suggests the possible existence of two aquifers; the boundary between them may be associated with the base of the low-velocity, increased porosity zone at 102.4 mbsf.

The total organic carbon content of the sediments was low, varying between 0.05% and 0.65%. Volatile hydrocarbons, with methane concentrations of 2 ppm and no detectable ethane or propane, presented no safety problems.

Shipboard paleomagnetic studies revealed a good reversal stratigraphy in the upper part of the section, registering the Matuyama/Gauss boundary at 54 mbsf (2.47 Ma). Below this level, the paleomagnetic reversal signal should be resolvable with the shore-based study of discrete samples.

## BACKGROUND AND SCIENTIFIC OBJECTIVES

Site 813 is one of three sites in close proximity along the southern margin of the Queensland Trough. For a summary of the background and overall objectives of these sites the reader is referred to the "Background and Scientific Objectives" section of the "Site 812" chapter (this volume). The location of Site 813 is shown on a track map of site survey data in Figs. 1 and 2.

The objectives for Site 813 were as follows:

1. To determine whether seismic geometries are related to sea level.
2. To determine the age of the reflectors that separate the aggradational and progradational units.
3. To determine whether shoreline signatures can be defined within the late onlapping facies.
4. To determine the age when the margin was drowned at this site.

## OPERATIONS

### Transit to Hole 813A

The transit from Site 812 (NEA-10A/1) to Site 813 (NEA-10A/3) covered 6.2 nmi in 5.25 hr at 1.2 kt average speed (in dynamic positioning mode). Pipe was pulled during the transit, the jars were serviced, and the RCB BHA was stood back in the derrick for future use. The 11-7/16-in. bit, APC/XCB BHA, monel drill collar (DC), and Hydrolex jars were run in to 474 m below rig floor (mbrf) in transit. A Datasonics commandable recall beacon was dropped off location by mistake at 0150L (all times are given in local time, or L) 24 August. A beacon was swung out with the release line tied to the ship. The ship could not offset to the required site, so a second beacon was dropped at 0315L within an optimal global positioning system (GPS) window at the previously surveyed GPS coordinates.

### Hole 813A

The precision depth recorder (PDR) indicated that the water depth at the site was 539.3 m from sea level. We ran the bit in to a water depth of 535 m, and Hole 813A (NEA-10A/3) was spudded at 0428L, 24 August, at a position of 17°49.959′S, 149°29.669′E. From first core, we recovered 5.72 m of sediments, placing the mud line at a depth of 539.1 m from sea level. Continuous APC cores (Cores 133-813A-1H to -21H) were taken from 0 to 192.7 mbsf, with 192.7 m cored and 198.36 m recovered (102.94%). Core 133-813A-21H was a partial stroke. Continuous XCB cores (Cores 133-813A-22X to -26X) were taken from 192.7 to 231.5 mbsf, with 38.8 m cored and 1.19 m recovered (3.07%). Poor XCB core recovery led to a trial run with the vibrapercussive coring tool (VPC) for Core 133-813A-24V. However, the VPC was apparently run on a hard ledge and had no penetration or recovery.

After dropping the XCB core barrel for Core 133-813A-27X, the drill string became stuck. Gel sweeps were pumped to clean the hole, but the pipe was freed repeatedly only to become stuck again in a notched "keyseat" above the jars. The pipe was worked from 193 to 222 mbsf, with 270,000 lb maximum overpull (230,000 lb string weight). Coring was ended due to hole problems and we pulled out of the hole. The seafloor was cleared at 1900L 24 August.

### Hole 813B

The ship was moved 25 m east, and Hole 813B was spudded at 2013L 24 August, at a water depth of 538.9 m, and a position of 17°49.951′S, 149°29.673′E. Continuous APC cores (Cores 133-813B-1H to -19H) were taken from 0.0 to 179.5 mbsf, with 179.5 m cored and 185.37 m recovered (103.27%). Cores 133-813A-4H through -19H were oriented.

We took VPC cores (Cores 133-813B-20V to -21V) from 179.5 to 190.0 mbsf, with 10.5 m cored and 10.79 m recovered (102.76% recovery). Core 133-813B-21V apparently hit refusal. The APC/XCB BHA was pulled up and cleared the seafloor at 0835L, 25 August. The bit was pulled to a water depth of 410 m for transit. A beacon was dropped by mistake, recalled, and recovered. The ship departed Site 813.

The coring summary for Site 813 appears in Table 1.

## SITE GEOPHYSICS

A general description of the design and operation of the joint site location survey for Sites 812, 813, and 814 is included in the "Site Geophysics" section of "Site 812" chapter (this volume).

### Site 813

Following completion of drilling at Site 812 and separation from the beacon at JD 235/1023UTC on 23 August 1990, the *JOIDES Resolution* returned to the confirmed GPS position of Site 813 in dynamic positioning mode, trailing the drill string. The first beacon was dropped at the site at JD 235/1550UTC; final coordinates of Hole 813A are 17°49.959′S and 149°29.669′E, with a water depth of 539.1 m (drill-pipe measurement, or DPM, from sea level).

Site 813 is located near the southern margin of Queensland Plateau, between Tregrosse and Flinders reefs, about 65 km west of the edge of the modern Tregrosse Reef bank (Fig. 1). This site is the most westerly of a group of three sites (Sites 812, 813, and 814) positioned so as to examine factors con-

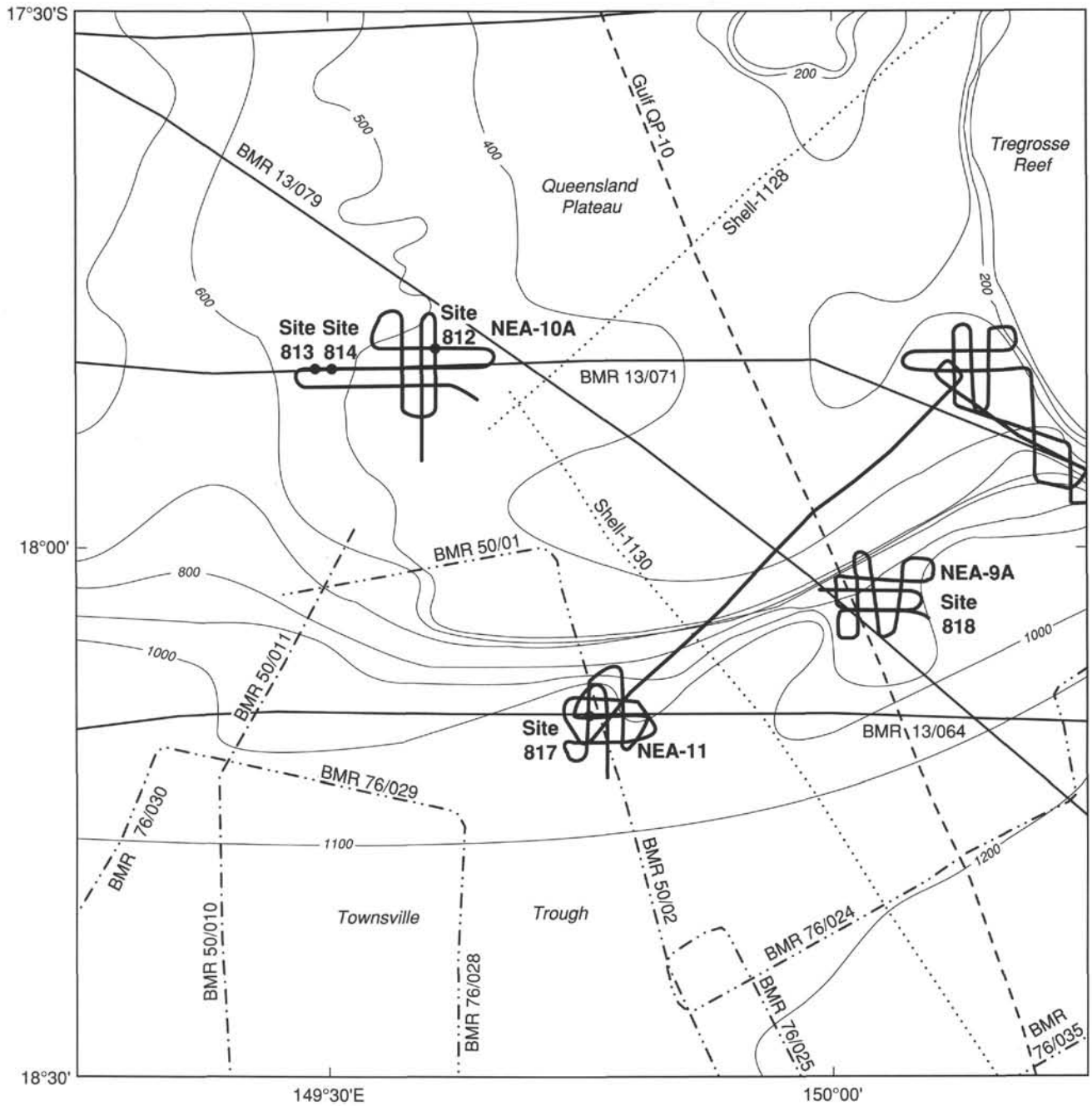


Figure 1. Track chart showing distribution of regional seismic data around Sites 812, 813, and 814 with Site 817 and Site 818 locations. Simplified bathymetry in meters.

trolling the development of carbonate platforms on the Queensland Plateau. Site 813 represents the most distal part of a prograding platform margin system and lies a little more than 5 km west of the edge of the platform (Fig. 2).

Correlation was good at the site between the two intersecting *JOIDES Resolution* single-channel seismic profiles and the *Rig Seismic* multichannel seismic profile (Figs. 1 and 3). Six seismic sequences can be recognized above the top of a strong band of reflectors about 0.5 s TWT (two-way traveltime) below seafloor. A strong reflector about 1.1 s TWT below seafloor, visible on both the processed BMR water-gun site survey data and other regional data in the area, may mark either the top of basement or the rift-fill section. It probably corresponds to the so-called regional Paleocene breakup unconformity, which is thought to have formed following the start of seafloor spreading in the Coral Sea Basin and consequent thermal sag of the continental margin (Falvey and Mutter, 1981; Symonds et al., 1984).

The character of the six seismic sequences at Site 813 is illustrated in Figure 3. The basal sequence S6 is about 0.13 s TWT thick and lies beneath TD. It is onlapped by the overlying sequence S5 (0.04 s TWT thick), which also occurs below TD and which consists of relatively low-amplitude disrupted reflectors. TD at Site 813 occurs within the overlying composite sequence S4 (0.07 s TWT thick), which contains high-amplitude reflectors that define a series of complex

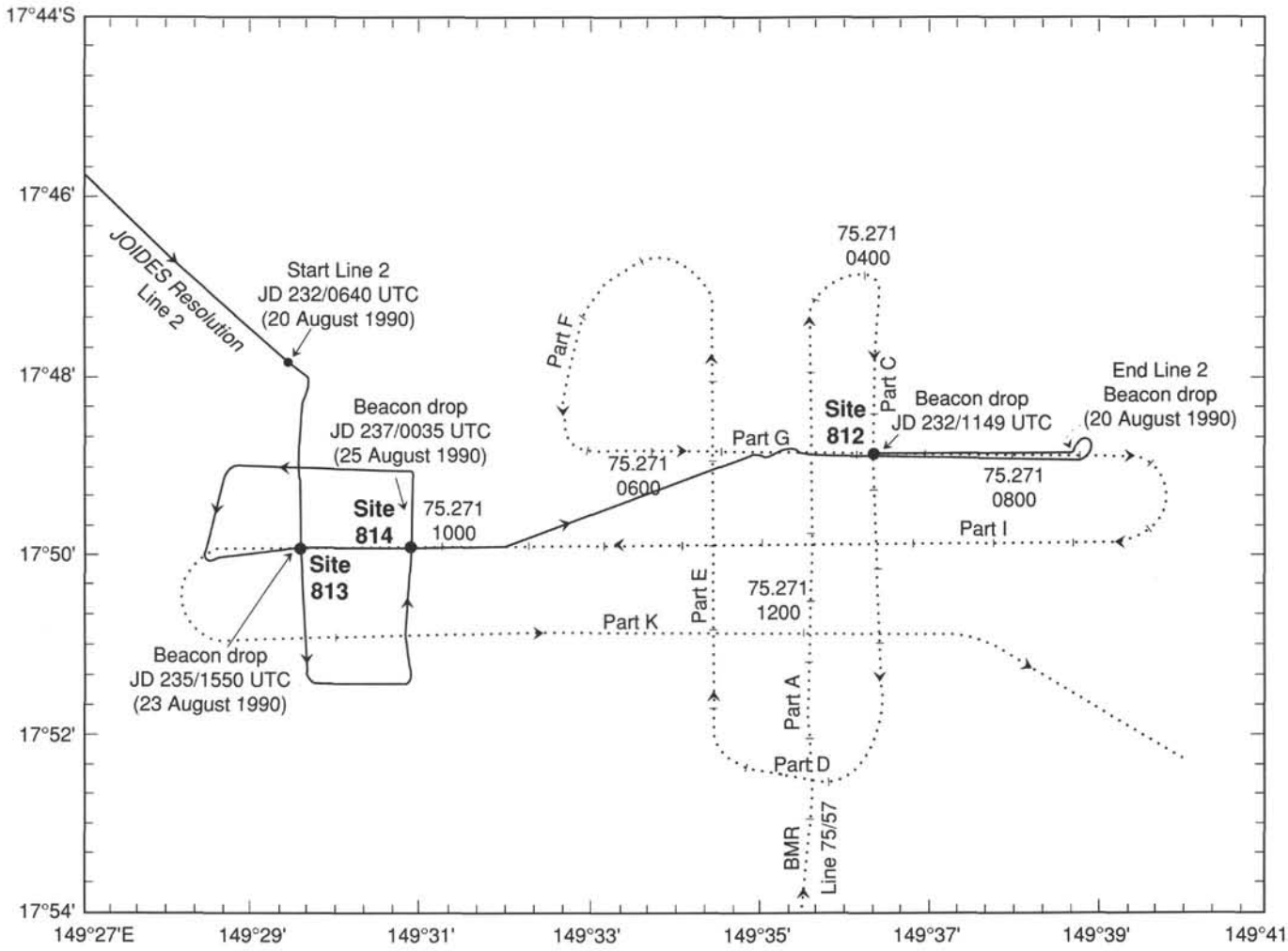


Figure 2. Detail of *JOIDES Resolution* Leg 133 site location tracks (solid Line) and *Rig Seismic* 1987 site survey tracks (dotted line) around Sites 812, 813, and 814.

onlapping and offlapping units, some of which have erosionally truncated upper surfaces. Sequence S3 (0.05 s TWT thick), which exhibits some truncation at its top, is mainly aggradational. Its upper surface is the most distinctive sequence boundary at Site 813. The overlying onlapping sequence S2 has a thickness of about 0.04 s TWT at the site, but rapidly pinches out to the east. The upper sequence S1 (0.08 s TWT thick) gently onlaps the underlying sequence and consists of low-amplitude subparallel reflectors. The pre-drilling interpretation (Fig. 3), which was based on an extrapolation of the prognosis for proposed site NEA-10A/2 (Site 814) (Feary et al., 1990) suggested that the upper two sequences are Quaternary to Pliocene pelagic and periplatform sediments and upward-fining transgressive units; the two middle sequences are late Miocene grainstones and packstones that were deposited in the outer part of a prograding reef slope; and the two basal sequences are early Miocene wackestone, packstone, and mudstone associated with carbonate platform build-up.

To provide some predictive capability during drilling at Site 813, we estimated the TWT/depth relationship below the seafloor using stacking-derived interval velocities from a BMR seismic line across the site (Fig. 4). At depths greater than 100 mbsf, velocities of sediments at Site 813 are higher than those for Site 811 and DSDP Site 209 (Andrews, 1973). This probably reflects the carbonate platform setting of Site 813.

## LITHOSTRATIGRAPHY

Site 813 lies on the southwestern margin of the extensive Tregrosse/Lihou/Coringa Bank complex, which makes up about 15% to 20% of the surface of Queensland Plateau. The location of this site, adjacent to the bank complex but in a distal location compared to Sites 812 and 814, suggests that the sequence should contain a mixture of bank-derived and pelagic materials.

During double APC drilling, we recovered complete sections to refusal depth at 190 mbsf (Fig. 5). With further drilling using the XCB in Hole 813A to 231.5 mbsf, we recovered only fragments of rock. Lithologies encountered during APC drilling were essentially homogeneous calcareous oozes, or their more lithified chalk equivalents, with variable proportions of micrite, foraminifers, nannofossils, and bioclasts. Five lithologic units were identified: Unit I is characterized by homogeneous ooze; Unit II by the presence of darker-colored, sand-sized grains; Unit III by homogeneous ooze; Unit IV by a much greater proportion of partially lithified or lithified chalk; and Unit V by fragments of dolomitized rock. Partially lithified, "chalky" bands occur throughout the calcareous ooze in Units I through III. Higher concentrations of these "chalky" bands in some intervals may have produced many of the low-amplitude reflectors visible throughout the site-

**Table 1. ODP coring summary.**

| Core no. | Date (Aug. 1990) | Time (UTC) | Depth (mbsf) | Length cored (m) | Length recovered (m) | Recovery (%) |
|---|---|---|---|---|---|---|
| Hole 813A | | | | | | |
| 1H | 22 | 1840 | 0–5.7 | 5.7 | 5.72 | 100.0 |
| 2H | 22 | 1855 | 5.7–15.2 | 9.5 | 9.87 | 104.0 |
| 3H | 22 | 1910 | 15.2–24.7 | 9.5 | 9.87 | 104.0 |
| 4H | 23 | 1935 | 24.7–34.2 | 9.5 | 9.88 | 104.0 |
| 5H | 23 | 2010 | 34.2–43.7 | 9.5 | 9.85 | 103.0 |
| 6H | 23 | 2030 | 43.7–53.2 | 9.5 | 10.05 | 105.8 |
| 7H | 23 | 2055 | 53.2–62.7 | 9.5 | 10.12 | 106.5 |
| 8H | 23 | 2115 | 62.7–72.2 | 9.5 | 9.01 | 94.8 |
| 9H | 23 | 2145 | 72.2–81.7 | 9.5 | 9.94 | 104.0 |
| 10H | 23 | 2205 | 81.7–91.2 | 9.5 | 9.17 | 96.5 |
| 11H | 23 | 2240 | 91.2–100.7 | 9.5 | 8.71 | 91.7 |
| 12H | 23 | 2305 | 100.7–110.2 | 9.5 | 9.62 | 101.0 |
| 13H | 23 | 2320 | 110.2–119.7 | 9.5 | 9.71 | 102.0 |
| 14H | 23 | 2343 | 119.7–129.2 | 9.5 | 9.78 | 103.0 |
| 15H | 24 | 0005 | 129.2–138.7 | 9.5 | 9.88 | 104.0 |
| 16H | 24 | 0030 | 138.7–148.2 | 9.5 | 9.88 | 104.0 |
| 17H | 24 | 0050 | 148.2–157.7 | 9.5 | 9.90 | 104.0 |
| 18H | 24 | 0110 | 157.7–167.2 | 9.5 | 9.91 | 104.0 |
| 19H | 24 | 0130 | 167.2–176.7 | 9.5 | 9.87 | 104.0 |
| 20H | 24 | 0155 | 176.7–186.2 | 9.5 | 9.80 | 103.0 |
| 21H | 24 | 0900 | 186.2–195.7 | 9.5 | 7.70 | 81.0 |
| 22X | 24 | 0340 | 195.7–202.4 | 6.7 | 0.59 | 8.8 |
| 23X | 24 | 0420 | 202.4–212.1 | 9.7 | 0.05 | 0.5 |
| 24V | 24 | 0550 | 212.0–212.1 | 0.1 | 0.00 | 0.0 |
| 25X | 24 | 0625 | 212.1–221.8 | 9.7 | 0.23 | 2.4 |
| 26X | 24 | 0650 | 221.8–231.5 | 9.7 | 0.32 | 3.3 |
| Coring totals | | | | 231.6 | 199.43 | 86.1 |
| Hole 813B | | | | | | |
| 1H | 24 | 1020 | 0.0–8.5 | 8.5 | 8.58 | 101.0 |
| 2H | 24 | 1035 | 8.5–18.0 | 9.5 | 9.24 | 97.2 |
| 3H | 24 | 1055 | 18.0–27.5 | 9.5 | 9.89 | 104.0 |
| 4H | 24 | 1120 | 27.5–37.0 | 9.5 | 9.94 | 104.0 |
| 5H | 24 | 1140 | 37.0–46.5 | 9.5 | 9.30 | 97.9 |
| 6H | 24 | 1205 | 46.5–56.0 | 9.5 | 9.93 | 104.0 |
| 7H | 24 | 1230 | 56.0–65.5 | 9.5 | 9.79 | 103.0 |
| 8H | 24 | 1250 | 65.5–75.0 | 9.5 | 10.06 | 105.9 |
| 9H | 24 | 1325 | 75.0–84.5 | 9.5 | 10.03 | 105.6 |
| 10H | 24 | 1350 | 84.5–94.0 | 9.5 | 9.80 | 103.0 |
| 11H | 24 | 1420 | 94.0–103.5 | 9.5 | 9.58 | 101.0 |
| 12H | 24 | 1545 | 103.5–113.0 | 9.5 | 9.28 | 97.7 |
| 13H | 24 | 1605 | 113.0–122.5 | 9.5 | 10.10 | 106.3 |
| 14H | 24 | 1625 | 122.5–132.0 | 9.5 | 9.91 | 104.0 |
| 15H | 24 | 1650 | 132.0–141.5 | 9.5 | 9.96 | 105.0 |
| 16H | 24 | 1715 | 141.5–151.0 | 9.5 | 9.91 | 104.0 |
| 17H | 24 | 1750 | 151.0–160.5 | 9.5 | 10.05 | 105.8 |
| 18H | 24 | 1805 | 160.5–170.0 | 9.5 | 9.97 | 105.0 |
| 19H | 24 | 1825 | 170.0–179.5 | 9.5 | 10.05 | 105.8 |
| 20V | 24 | 1955 | 179.5–188.0 | 8.5 | 8.79 | 103.0 |
| 21V | 24 | 2125 | 188.0–190.0 | 2.0 | 2.00 | 100.0 |
| Coring totals | | | | 190.0 | 196.16 | 103.2 |

Note: Times are given in Universal Time Coordinated or UTC, which is 10 hr later than local time or L.

survey seismic section (see "Site Geophysics" section, this chapter; Fig. 3).

## Lithologic Units

***Unit I (Sections 133-813A-1H-1 through -9H-4 and 133-813B-1H-1 through -9H-2; depth, 0–76.8 mbsf; age, Pleistocene to Pliocene)***

Unit I consists of essentially homogeneous, micrite foraminifer to foraminifer nannofossil ooze with bioclasts. The variations in relative proportions of micrite and nannofossils appear to be gradational, with no obvious bedding. A subtle light/dark color alternation (very white to white) is visible in the uppermost 30 m of this unit (Sections 133-813B-1H-1 through -3H-4, and may reflect increases in the relative proportion of nannofossils and decreases in the proportion of micrite in the lighter zones. Elsewhere, the color is a uniform very white to white, except in the basal 18 m of the unit, where bands and irregular "blebs" of pink to very light brown tinted ooze become more apparent toward the base. Patches of partially lithified, slightly more "chalky" ooze occur throughout the unit. The irregular shape and distribution of "chalky" lumps is most probably a real feature, although some disruption may have resulted from drilling and core handling procedures. Increased concentrations of partially lithified material were noted at ~53 mbsf (Sections 133-813A-6H-6 to -6H-7 and 133-813B-6H-5) and 70 mbsf (Sections 133-813A-8H-4 to -8H-5 and 133-813B-8H-4).

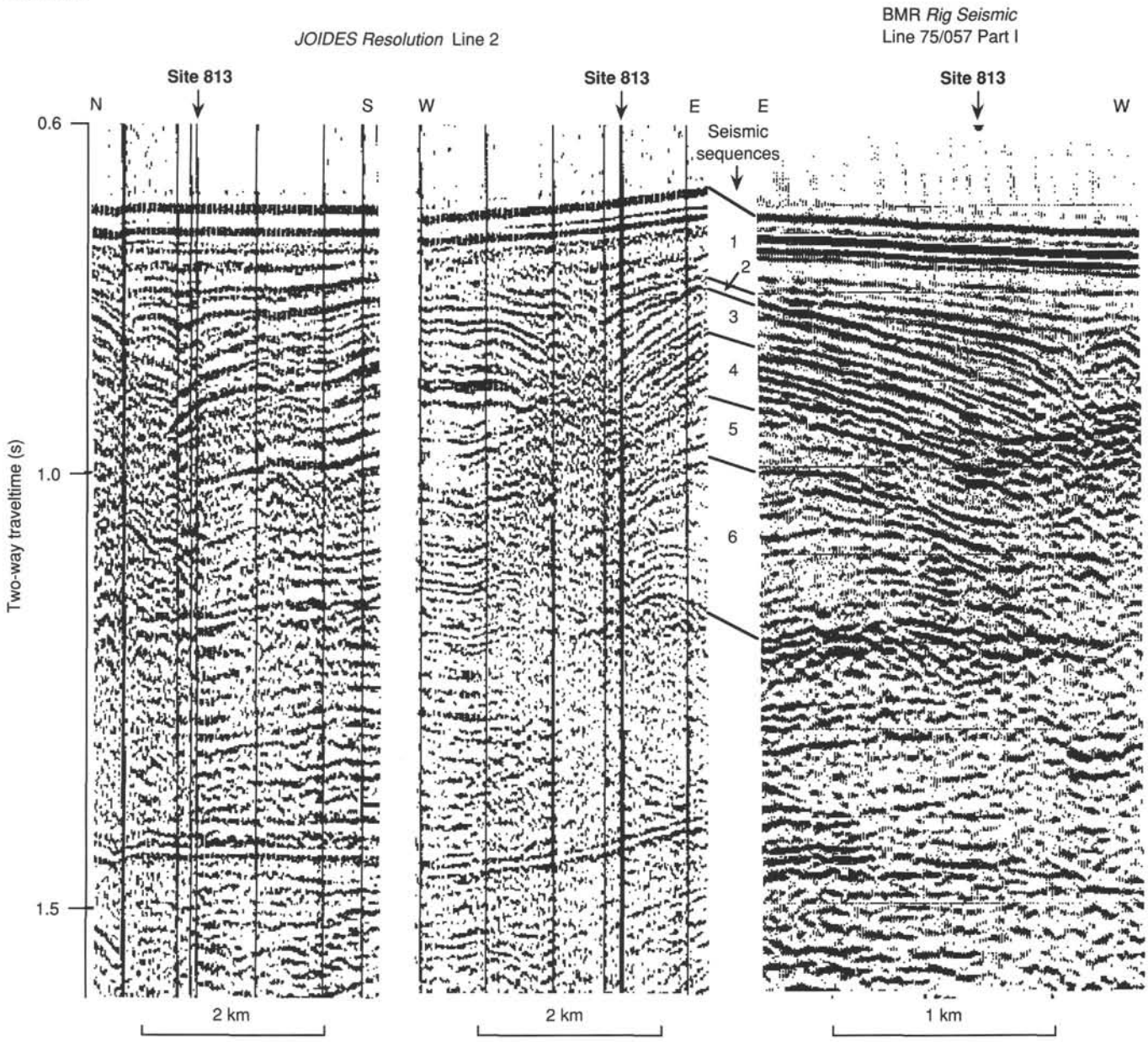


Figure 3. Comparison of *JOIDES Resolution* and *Rig Seismic* 80-in.$^3$ water-gun seismic profiles across Site 813. Also shown is the characteristics of sequences in the *Rig Seismic* seismic profile across the site (S1, S2, etc.).

***Unit II (Sections 133-813A-9H-4 through -13H-5 and 133-813B-9H-2 through -13H-3; depth, 76.8–117 mbsf; age, Pliocene to late Miocene)***

Unit II is a white to very pale brown, nannofossil foraminifer ooze with micrite. The most distinctive characteristic of this unit is the presence of darker colored, sand-sized, iron-stained and/or phosphatized grains variably distributed throughout the unit (Fig. 6). Dark reddish-brown to reddish-yellow grains, consisting of cemented lithoclasts, benthic foraminifers, bioclastic fragments, and unidentifiable grains, occur within the uppermost 13 m of the unit (Sections 133-813A-9H-4 through -10H-7 and 133-813B-9H-2 through -10H-5). The proportion of these grains increases in the basal 0.5–1 m of Unit I; reaches a maximum in the top 1–2 m of Unit II; and decreases gradually throughout the underlying 12 m. The zone containing brown grains is underlain by 9 m of nannofossil foraminifer ooze containing little or no dark grains. The basal 18 m of the unit (Sections 133-813A-11H-5 through -13H-5 and 133-813B-12H-1 through -13H-3) contains gray, phosphatized, and often partially corroded benthic foraminifers. The proportion of these grains reaches a maximum of close to 10% of the sediment ~8 m above the base of Unit II (Section 133-813B-12H-4). The remainder of the sand fraction in Unit II is predominantly white, planktonic foraminifers. Partially lithified "chalky" lumps occur irregularly distributed throughout the unit, but with greater concentrations in poorly defined bands at ~87 mbsf (Section 133-813A-10A-3) and 97 mbsf (Sections 133-813A-11H-2 to -11H-3). The proportions of sand- and mud-sized components vary throughout the unit, although without clear boundaries, and in some places may represent indistinct upward-fining cycles.

The uppermost 2–3 m of Unit II contains increasing proportions of irregular pinkish-white bands, with coloration increasing up to the 20-cm-thick, slightly more lithified sandier layer that marks the top of the unit. GRAPE data show that

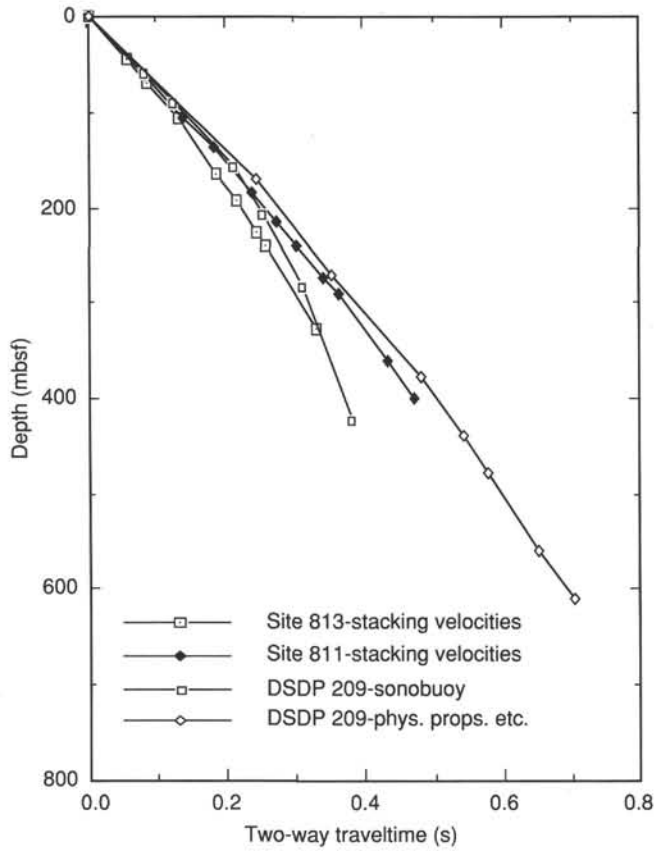


Figure 4. Comparison of reflection time (TWT)-depth curve estimated for Site 813 with those for Site 811 and DSDP Site 209 on the Queensland Plateau.

this boundary is also marked by an abrupt jump in wet-bulk density from ~1.65 to 1.75 g/cm$^3$ (see "Physical Properties" section, this chapter).

***Unit III (Sections 133-813A-13H-5 through -17H-CC and 133-813B-13H-3 through -17H-6; depth, 117–160 mbsf; age, late Miocene)***

Unit III is a homogeneous, white, predominantly unlithified bioclastic foraminifer ooze with micrite and nannofossils. Partially lithified "chalky" lumps, ranging from granule-sized to the entire core width, occur irregularly distributed throughout the unit, but with greater concentrations in poorly defined bands at ~118 mbsf (Section 133-813A-13H-5/6), 133 mbsf (Section 133-813B-15H-1), and 154 mbsf (Section 133-813B-17H-3). Slight variations in the proportions of sand- and mud-sized components throughout the unit may reflect indistinct upward-fining cycles. One clear occurrence of darker colored mottling toward the base of the unit (Section 133-813A-17A-6; 156 mbsf), <12.62 cm across and ≤10 cm long, presumably represents bioturbation.

***Unit IV (Sections 133-813A-18H-1 through -22X-CC and 133-813B-17H-7 through -21V-CC; depth, 160–~195 mbsf; age, late Miocene to middle Miocene)***

The basal 3 m of Unit IV consists of white, dolomitized, bioclastic nannofossil chalk interbedded with 4– to 10-cm-thick beds of white to very pale brown, unlithified, dolomite lithoclast foraminifer rudstone and packstone. The remainder of the unit consists of very white to very pale brown, semilithified to lithified dolomite foraminifer micrite chalk with bioclasts, interbedded with unlithified to partially lithified, very white to white, dolomite micrite foraminifer ooze with bioclasts and nannofossils. The dolomite component may have been reworked as both dolomite grains and/or unabraded dolomite crystals. The fragments and "biscuits" of chalk occurring in the core, commonly ~10 cm thick, are likely to represent thin, irregular chalk beds, which have been disrupted by drilling. Two ~80-cm-thick beds of partly lithified foraminifer packstone occur at ~170 mbsf (Sections 133-813A-19H-2 to -19H-3).

***Unit V (Sections 133-813A-23X-1 through -26X-1; depth, ~195–231 mbsf; age, middle Miocene or older)***

Unit V is represented only by a number of lithified, completely dolomitized fragments with extensive intercrystalline porosity, and accordingly it is impossible to determine the extent to which the small amount of recovered material is representative of the cored interval. The fragments in Section 133-813A-23X-CC (from within the range 203–212 mbsf) and Section 133-813A-26X-1 (from within the range 222–231 mbsf) are too altered by dolomitization to determine the original depositional facies. The fragments in Section 133-813A-25X-CC (from within the range 213–222 mbsf) are dolomitized skeletal grainstone fragments with extensive moldic and intercrystalline porosity. As a result of the extensive dolomitization, the only recognizable skeletal elements are calcareous algae and foraminifers.

## Interpretation

Although the APC section to 190 m (Units I–IV) is predominantly homogeneous calcareous ooze, the combination of facies type and the broad paleodepth indications provided by benthic foraminifer studies (see "Biostratigraphy" section, this chapter) make it possible to draw a number of generalized conclusions regarding depositional environments and processes. The dolomitized grainstone fragments in Unit V, together with the indications of shallow neritic paleodepth from benthic foraminifers, suggests that this unit was either deposited adjacent to or within a carbonate bank. The coarse-grained beds at the base of Unit IV probably represent sediment gravity flow deposition in a relatively shallow (shallow neritic) environment adjacent to the carbonate bank. The presence of these coarser grained beds within the lower part of this unit only, combined with an increase in the pelagic component higher in the unit, indicates either an increasingly low energy, distal position relative to the carbonate bank or a more restricted supply of coarse material. Unit III represents the combined effects of pelagic deposition together with the introduction of bank-derived micritic material. The decreased bank-derived component, relative to Unit IV, indicates increased isolation from the shallow carbonate bank. The continued evidence of outer neritic to upper bathyal water depths from benthic foraminifers and the characteristic presence of reworked phosphatized and/or ferruginized grains throughout most of Unit II, including lithoclasts and transported reefal benthic foraminifers (see "Biostratigraphy" section, this chapter), suggests that this site was receiving eroded fragments from a source characterized by negligible sedimentation rate and chemical alteration. The hardground surface drilled at 57 mbsf in Site 814 (Section 133-814A-8H-1) is a possible source for this reworked material. Unit II therefore represents a more expanded, but nevertheless still condensed section reflecting a sea-level rise dated as late Miocene–early Pliocene from available biostratigraphy (see "Biostratigraphy" section, this chapter). The possible presence of upward-fining cycles within Unit II indicates that sediment gravity flow deposition may have provided the mechanism for supplying

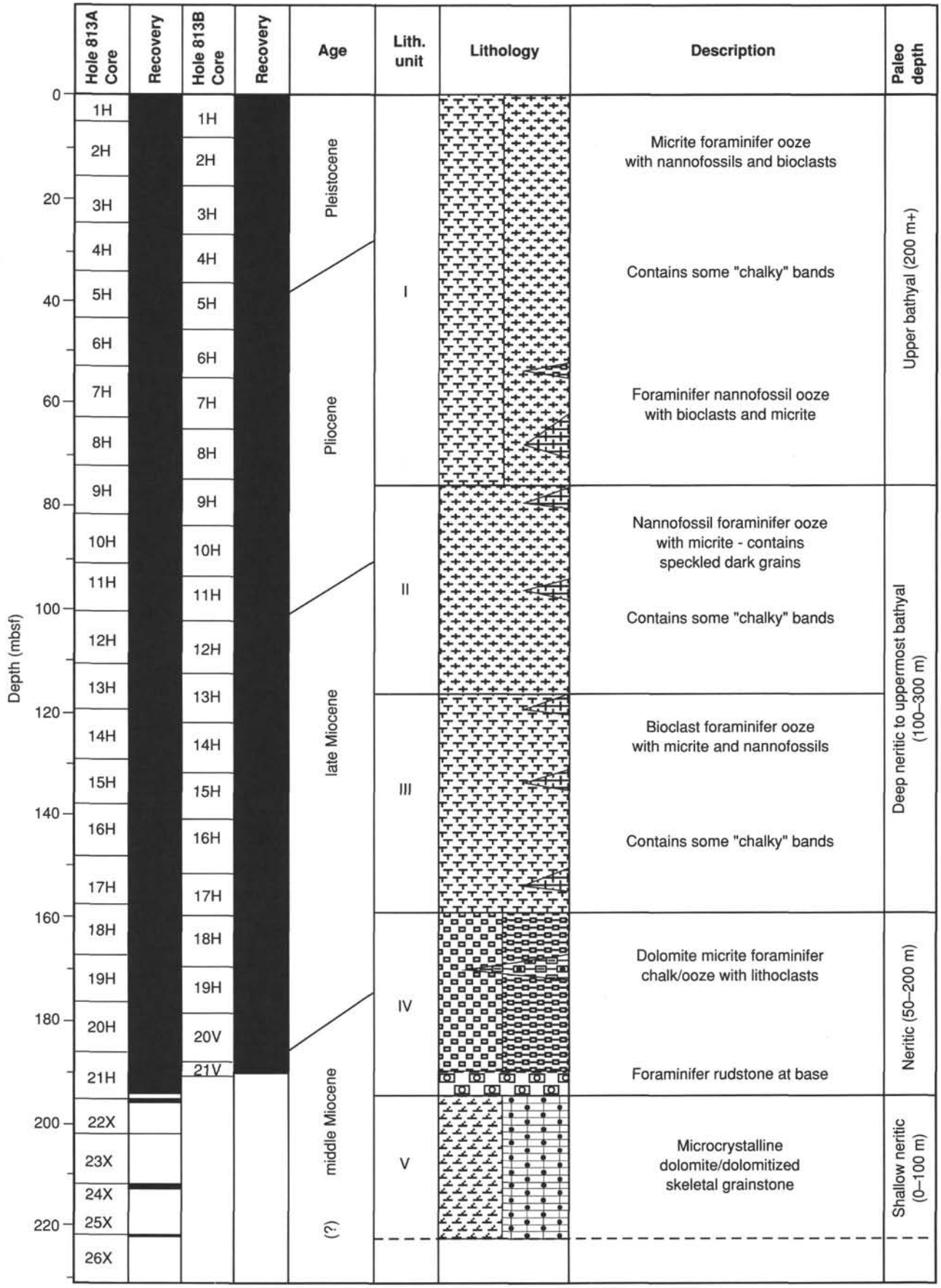


Figure 5. Summary chart showing the lithology for each lithologic unit identified at Site 813. Biostratigraphic and paleodepth data are from analysis of benthic foraminifer, planktonic foraminifer, and nannofossil associations (see "Biostratigraphy" section, this chapter). Lithological patterns are from the "Explanatory Notes" chapter (this volume).

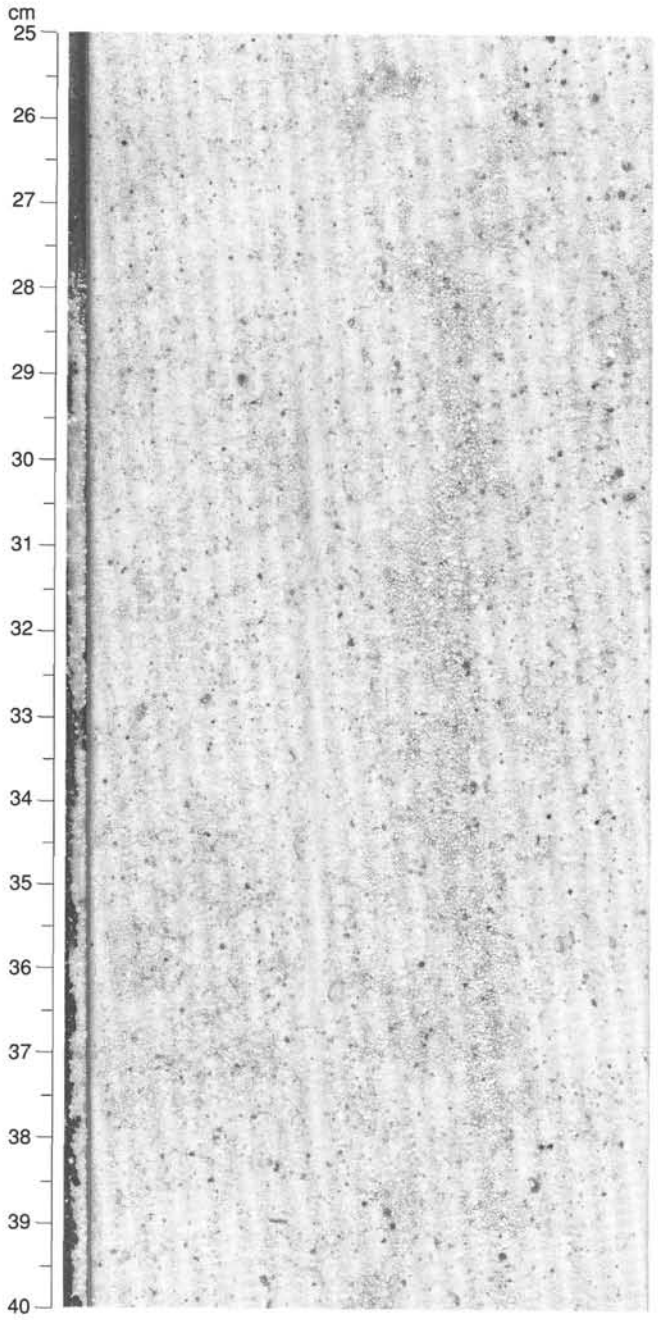


Figure 6. Photograph of 25–40 cm in Section 133-813A-9H-7 showing darker colored, ferruginized and/or phosphatized grains distributed throughout white, nannofossil foraminifer ooze.

these reworked grains, although the absence of clear boundaries and the relatively even distribution of the darker grains throughout most of the Unit II cores would indicate that there must have been extensive *in-situ* reworking or current redeposition. The significance of the different types of reworked grains (gray phosphatized benthic foraminifers at the base; brown abraded grains toward the top) is not clear, and must await more detailed lithologic and biostratigraphic analysis of this interval from this site and from Sites 812 and 814. The abrupt cessation of the supply of reworked material at the base of Unit I suggests that a relative sea-level rise curtailed the erosion or supply processes, with the result that deposition of Unit I occurred with the accumulation of both pelagic and fine-grained, bank-derived, periplatform material. A greater understanding of the relative importance of the pelagic and periplatform depositional processes, and the extent to which the lithologic variation is a function of glacial/interglacial cyclicity, must await more detailed studies of the relative contributions and ages of the fine-grained components.

## BIOSTRATIGRAPHY

### Biostratigraphy and Paleoenvironment Synthesis

Calcareous nannofossils and planktonic, benthic, and larger benthic foraminifers were extracted from core-catcher samples from Holes 813A and 813B. An overview of the biostratigraphic results is given in Figure 7. Planktonic fossils are abundant in the upper part of the section. The microfossils are generally well preserved, however preservation deteriorates downward because of overgrowth. The lowermost sample with datable planktonic fossils (133-813A-12H-CC) is late Miocene. The first appearance of larger benthic foraminifers in Sample 133-813A-20H-CC suggests a middle Miocene age for this sample. The benthic foraminiferal associations indicate a change from an inner to middle neritic depositional environment in the lower part of the section to an upper bathyal environment in the middle and upper part (Fig. 8).

### Calcareous Nannofossils

All core-catcher samples from Hole 813A were examined for calcareous nannofossils. Nannofossils were recovered from Cores 133-813A-1H through -20H (0–186.2 mbsf). The interval represents a more or less continuous section from the upper Quaternary into the upper Miocene. Abundance of nannofossils ranges from 80% of the sediment in the lower Pleistocene (at 34.2 mbsf) and uppermost Pliocene (at 43.7 mbsf) to less than 1% in Sample 133-813A-21H-CC. Preservation of the nannofossils is fair to poor, and in general deteriorates with depth of burial. Overgrowth of fossils is common. Following is a summary of the nannofossil biostratigraphy, based mainly on core-catcher samples.

Sample 133-813A-1H-CC (5.7 mbsf) contains abundant *Gephyrocapsa caribbeanica*, but no *Emiliania huxleyi* or *Pseudoemiliania lacunosa;* it was assigned to CN14b, with an age range of 275 to 450 k.y. The next lower sample, 133-813A-2H-CC (15.2 mbsf) contains *Pseudoemiliania lacunosa* as well as abundant large *Gephyrocapsa* (*G. caribbeanica*); it was assigned to CN14a (450–930 k.y.). Sample 133-813A-3H-CC contains very rare large *Gephyrocapsa* and an overwhelming dominance of small specimens of *Gephyrocapsa*; hence, it was assigned to the middle Pleistocene interval of dominantly small *Gephyrocapsa* (0.93–1.27 Ma). This was followed in the next sample (133-813A-4H-CC) by *Calcidiscus macintyrei* (but without discoasters), which indicates an age of CN13a (1.48–1.88 Ma) for this stratigraphic level.

*Discoaster brouweri* occurs in the next lower sample (133-813A-5H-CC; 53.2 mbsf), followed by *Discoaster pentaradiatus, D. surculus,* and *D. asymmetricus* in Sample 133-813A-6H-CC (53.2 mbsf) for age ranges of 1.88–2.29 Ma and 2.42–2.60 Ma, respectively. The next two samples, 133-813A-8H-CC and -9H-CC, are both assigned to CN12a (2.60–3.45 Ma) based on the presence of *Discoaster tamalis* in the former and the absence of *Sphenolithus abies* in both. The last species, plus *Reticulofenestra pseudoumbilica* occur in Sample 133-813A-10H-CC (89.9 mbsf) and this sample is assigned to the lower Pliocene (CN10–CN11; 3.51–5.21 Ma).

Sample 133-813A-11H-CC yielded *Discoaster quinqueramus* and, accordingly, the Miocene/Pliocene boundary is within this core. *Discoaster quinqueramus* was recorded in Sample 133-813A-19H-CC, identifying this interval as the

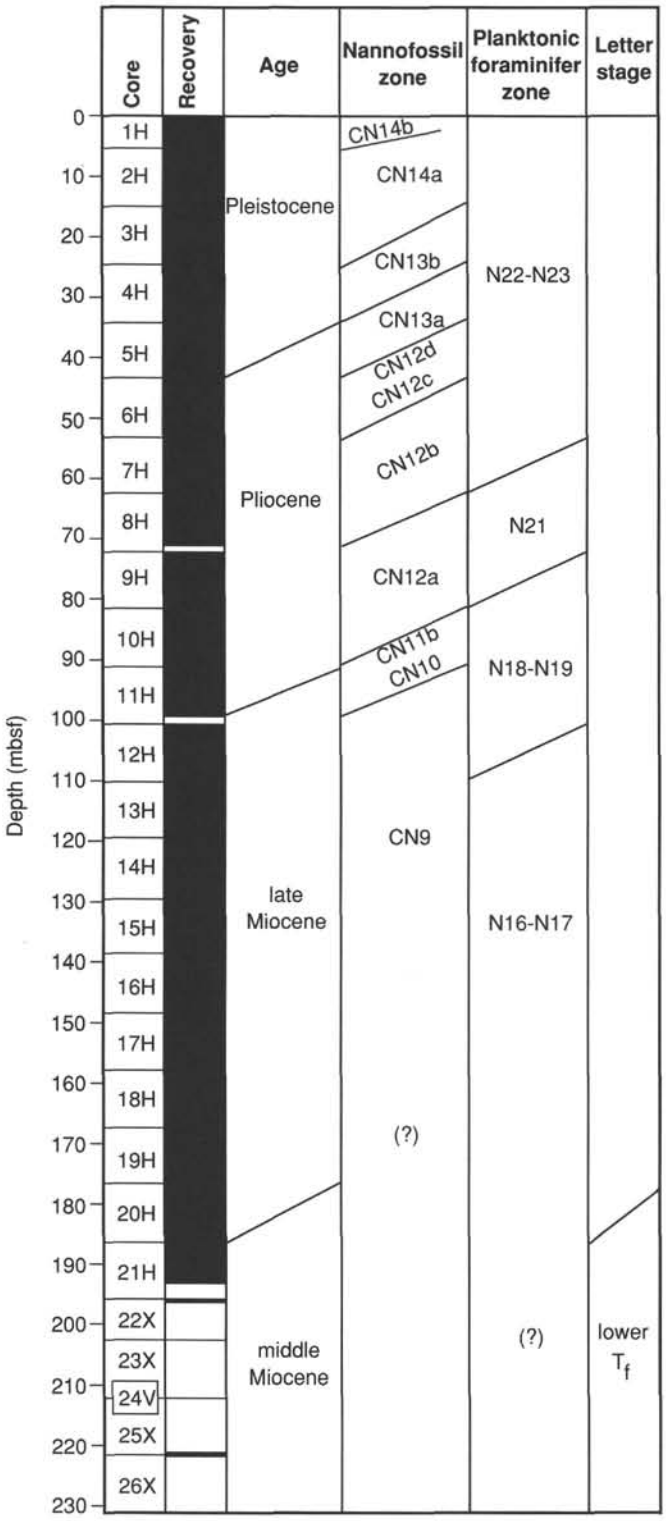


Figure 7. Overview of preliminary biostratigraphy of Site 813.

upper Miocene Zone CN9 (5.23–8.2 Ma); however, specimens recorded as *D. quinqueramus* in Samples 133-813A-18H-CC and -19H-CC might belong to *D. bellus* or *D. pentaradiatus*, the three being indistinguishable in these heavily overgrown assemblages. Sample 133-813A-20H-CC yielded abundant (but no age-diagnostic) nannofossils, and Sample 133-813A-21H-CC yielded very rare *Reticulofenestra* only. No nannofossils were recovered below Core 133-813A-21H.

## Planktonic Foraminifers

All core-catcher samples of Hole 813A were investigated for planktonic foraminiferal content. The Pliocene-Pleistocene section yielded well-preserved, abundant planktonic foraminifers. The lower part of the hole, which is referred to the late Miocene, has scattered occurrences of poorly preserved specimens.

The last occurrences of *Globigerinoides fistulosus* and *Globigerinoides obliquus* were encountered in Sample 133-813A-4H-CC, which indicates the lowermost part of the Pleistocene. The first occurrence of *Globorotalia truncatulinoides* is in Section 133-813A-6H-CC, which delineates the lower limit of Zone N22–N23. Below this biohorizon, we found the latest occurrences of *Globoquadrina altispira* (2.9 Ma) and *Sphaeroidinella seminulina* (3.0 Ma) in Sample 133-813A-8H-CC. The zonal boundary between N21 and N18–N19 is placed between Sections 133-813A-8H-CC and -9H-CC, based on the first occurrence of *Globorotalia tosaensis*. The first occurrence of *Globorotalia tumida tumida* in Sample 133-813A-11H-CC records the N18–N19 to N16–N17 zonal boundary. Below this level, the abundance of planktonic foraminifers diminishes and preservation deteriorates, which makes identification at the species level uncertain.

## Benthic Foraminifers

Preservation at Hole 813A is poor to moderate in and below Core 133-813A-13H, where benthic foraminifers are strongly recrystallized. Samples 133-813A-9H-CC through -20H-CC contain transported reefal benthic foraminifers mixed with *in-situ* benthic foraminiferal assemblages. Benthic foraminifers indicate a gradual deepening from the neritic (0–200 m) to upper bathyal (200–600 m) zones within the Pliocene.

Sample 133-813A-20H-CC contains the depth-diagnostic species *Cibicidoides matanzasensis* and *C. pachyderma*, but lacks the upper bathyal markers that were found in overlying samples, indicating a middle to outer neritic setting (30–200 m). Generally shallow-water taxa found in this sample include *Elphidium* spp., *Discorbis* spp., and *Discorbinella* spp.

Outer neritic to upper upper bathyal benthic foraminiferal assemblages characterize Samples 133-813A-13H-CC and -15H-CC. Sample 133-813A-15H-CC contains *Hyalinea balthica, Neoeponides campester, Sphaeroidina bulloides,* and abundant *Elphidium* spp. Sample 133-813A-13H-CC contains *Cibicidoides matanzasensis* and rare specimens of *Bulimina marginata, C. mundulus,* and *Uvigerina proboscidea.*

Sample 133-813A-12H-CC includes the taxa *Cibicidoides dutemplei, Hyalinea balthica,* and abundant *Elphidium.* In addition, rare specimens of *Hanzawaia mantaensis* were found. These taxa and the lack of exclusively bathyal benthic foraminiferal markers suggest that this sample was deposited in an outer neritic environment (100–200 m).

Sample 133-813A-9H-CC contains rare specimens of the bathyal species *Cibicidoides mundulus,* whereas abundant *C. pachyderma* are present. One specimen each of *Bulimina mexicana* and *Hanzawaia mantaensis* were found in this sample. *Cibicidoides dutemplei, Hyalinea balthica,* and *Uvigerina carapitana* are abundant. The benthic foraminiferal assemblage in Sample 133-813A-9H-CC indicates an outer neritic to upper upper bathyal paleodepth.

Samples 133-813A-1H-CC, -6H-CC, and 8H-CC contain upper bathyal (200–600 m) benthic foraminiferal assemblages, including the species *Bulimina marginata, B. mexicana, Cibicidoides dutemplei, C. mundulus, C. subhaidingerii, Planulina* sp. cf. *P. dohertyi,* and *Uvigerina proboscidea* (van Morkhoven et al., 1986). Sample 133-813A-1H-CC also con-

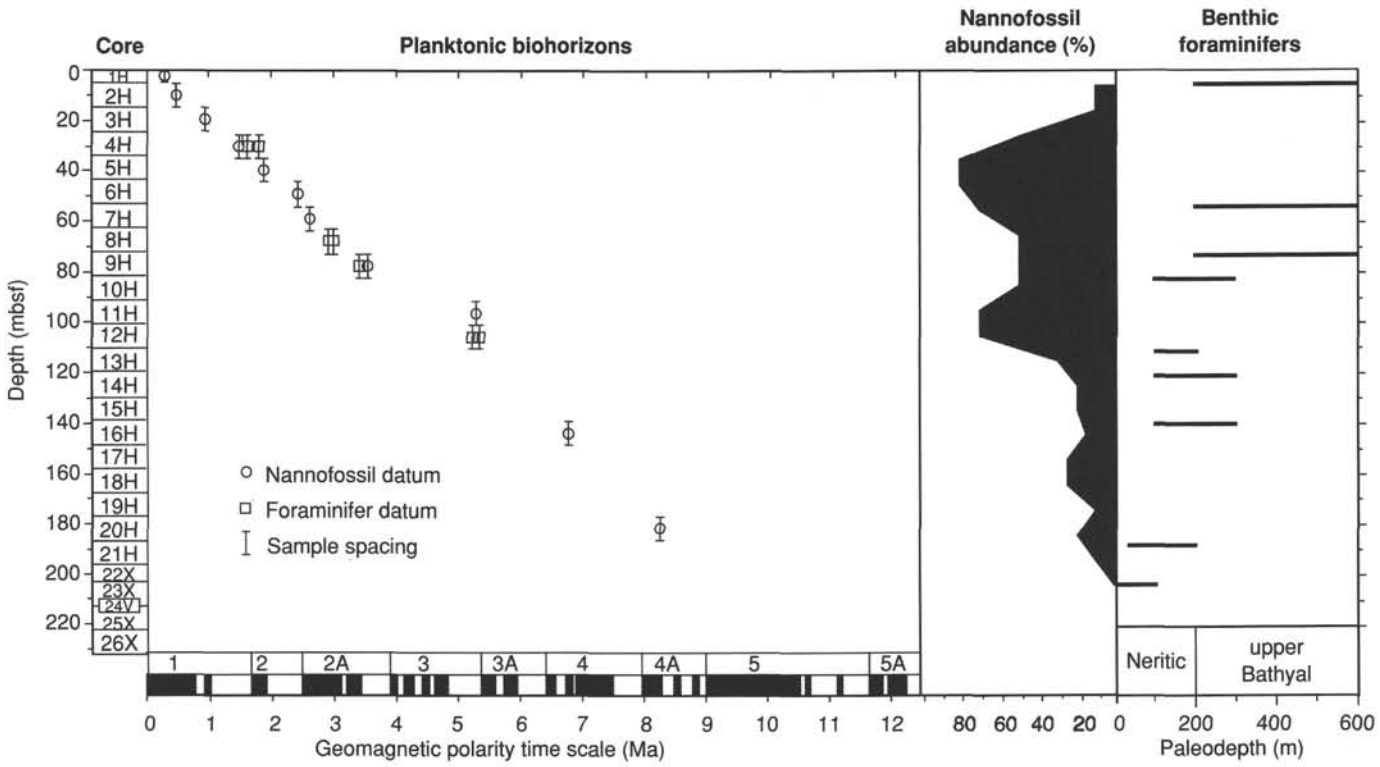


Figure 8. Sediment accumulation rate at Site 813. Nannofossil abundance and benthic foraminifer paleobathymetry are also shown.

tains abundant *Hoeglundina elegans*. Samples 133-813A-1H-CC and -6H-CC contain no reefal benthic foraminifers, whereas Sample 133-813A-8H-CC contains small, well-preserved specimens of transported reefal benthic foraminifers *Amphistegina* spp. and *Asterigerina* spp.

### Larger Benthic Foraminifers

Larger benthic foraminifers occur in Samples 133-813A-20H-CC through -22X-CC. In Sample 133-813A-20H-CC frequent lepidocyclinas (*Nephrolepidina martini*) were observed. The preservation is moderate and most of the specimens are strongly affected by microborings. Sample 133-813A-21H-CC contains rare lepidocyclinas and amphisteginid forms. Sample 133-813A-22X-CC contains *Gypsina globulus* (one specimen), rare *Cycloclypeus*, rare *Operculina*, rare to frequent amphisteginids, and frequent *Nephrolepidina martini* which indicates a middle Miocene age.

## PALEOMAGNETISM

Continuous archive-half NRM and AF 15-mT analyses were performed at Hole 813A from 0 to 195.7 mbsf and on Hole 813B from 0.0 to 56.0 mbsf. The reversal stratigraphy and precise boundaries were not well defined after the AF 15 mT step. However, several reversal zones (based on inclination changes) were apparent at Hole 813A that have been tentatively correlated to the geomagnetic polarity time scale with the aid of the core-catcher biostratigraphic markers. Below 50 mbsf, the inclination record becomes too scattered to interpret from shipboard data alone. The extension downward and refinement of the reversal stratigraphy will have to await discrete land-based sample analysis and refined biostratigraphic tie-points.

The preliminary magnetostratigraphy at Hole 813A is based on the reversal in inclination angles, measured from the archive-half of the core at 10-cm intervals. The normal and reversed zones still show considerable scatter, thus the reversal stratigraphy is not well defined and the boundaries identified during the shipboard phase are considered preliminary. With this in mind, the boundaries are placed at the following depths; Brunhes/Matuyama at ~17.0 mbsf, the top and bottom of the Jaramillo Subchron at ~20.0 and 23.0 mbsf, and the Olduvai Subchron from 37.8 to ~44 mbsf. The 2.47-Ma datum at the Matuyama/Gauss boundary was placed at ~55 to 56 mbsf, as inclinations are scattered across the reversal.

The average intensity of NRM magnetization is approximately 0.5 mA/m, while the upper 20 m often has moments greater than 2 mA/m. Below 20 mbsf, NRM intensities usually range between 0.3 and 1 mA/m. After 15 mT AF demagnetization, intensities decrease by about 40% to 50%. Comparison of NRM with AF 15-mT intensities plotted vs. depth show that remanence-carrying magnetic minerals are responding uniformly to AF demagnetization. However, stronger AF demagnetization will be necessary to remove the pervasive secondary normal overprint completely if possible. The high water contents and unconsolidated, coarse-grained nature of the sediments may have promoted remagnetization during drilling and handling aboard the ship.

Shipboard magnetic analyses of Hole 813B were performed on archive halves of the first six cores (133-813B-1H to -6H, 0–56.0 mbsf) because this interval in Hole 813A displayed several apparent polarity reversals. The preliminary magnetostratigraphic correlation was based solely on AF 15-mT inclination values and their change in orientation between the NRM and AF 15-mT levels. After AF demagnetization at 15 mT, zones of reversed polarity still contained some scattered normal inclinations, indicating insufficient AF demagnetization of a secondary component. Second, because no biostratigraphic markers were available for this core, reversal boundaries were constrained using Hole 813A biostratigraphy.

The Brunhes/Matuyama boundary was placed at about 16.5 mbsf. The Jaramillo Event was placed at ~19.5 to 22 mbsf. The Olduvai Subchron was not especially well defined at the

AF 15-mT demagnetization step and was only tentatively placed at ~36.8 to 42.5 mbsf. From ~43 to 54 mbsf, a scattered inclination record suggests that the interval may be of reversed polarity, but this will have to be assessed after demagnetization to higher levels for discrete samples. The Matuyama/Gauss boundary, representing the 2.47 Ma datum, was placed between 54 and 55 mbsf.

Continuous whole-core magnetic susceptibilities were measured for the top 195.7 m of Hole 813A (Fig. 9). Susceptibility values are generally near zero or slightly negative, indicating a low ferrimagnetic (magnetite) mineral content. From the top of the core to about 20 mbsf, a small peak in susceptibility occurs, perhaps suggesting minor influx of magnetite grains, either detrital or biogenic. By 20 mbsf, these ferrimagnetic grains have been either diagenetically altered or the magnetic sediment influx was considerably lower at the time of deposition. This susceptibility peak corresponds to the higher NRM and AF 15-mT intensities seen in the whole-core analyses. Likewise, a minor peak in susceptibility between about 64 and 90 mbsf corresponds with an increased NRM intensity at that level in the cryogenic record of the archive halves. These peaks may represent increased detrital influx because no sign of obvious diagenetic products, such as pyrrhotite or pyrite, were observed in the split cores.

To refine and expand the reversal stratigraphy, 273 oriented discrete samples were collected from Hole 813A. Because intensities were too weak to measure using the shipboard spinner magnetometer and because of a lack of time available for analyzing discrete samples with the cryogenic magnetometer, all samples will be analyzed at a shore-based laboratory.

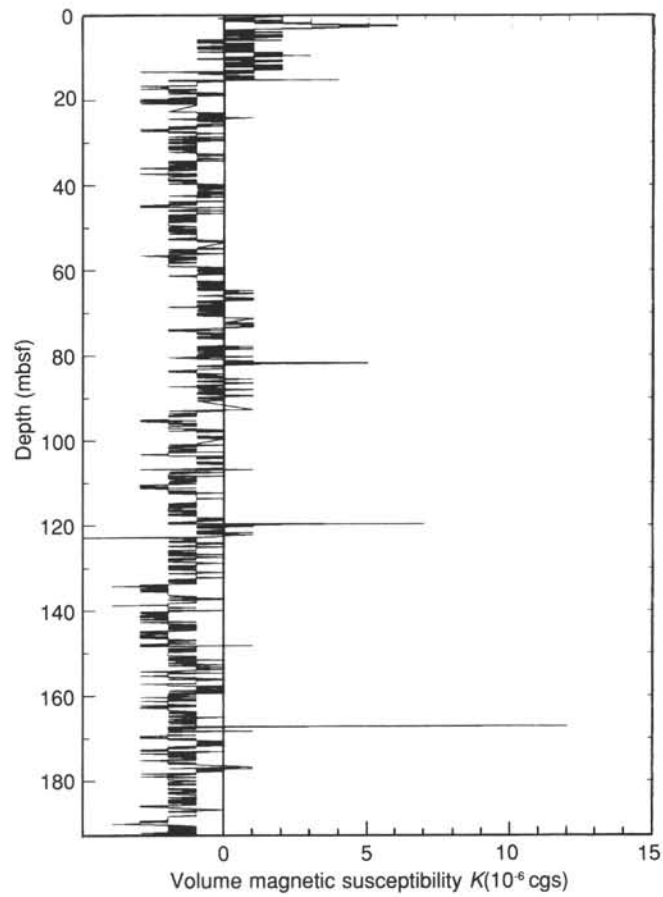


Figure 9. Continuous whole-core volume susceptibilities for Hole 813A. Weak susceptibility suggests that only a small concentration of ferrimagnetic grains (magnetite?) occur in this carbonate setting. Whole-round cryogenic intensity data show a weak remanence at the NRM and AF 15 mT levels.

## SEDIMENT ACCUMULATION RATES

Sediment accumulated at Site 813 at a fairly constant rate, within the resolution limits of the time framework based on core-catcher samples (see Fig. 8). From the Holocene to the middle Pliocene (0–3.5 Ma) sediment accumulated at about 2.2 cm/k.y. For the lower Pliocene (3.51–5.26 Ma) accumulation was at a significantly lower rate of only about 1.2 cm/k.y., but increased again to perhaps as much as 3 cm/k.y. in the uppermost upper Miocene. The lowermost dated sample, based on calcareous nannofossils (basal upper Miocene) projects onto a straight line and suggests a constant sedimentation rate for the upper Miocene.

The nannofossil abundance (pelagic vs. non-pelagic input into the sediment) does not seem to be related to the sedimentation rate. The paleobathymetry plot, however, indicates that the interval of reduced sediment accumulation corresponds to the time when water depth increased markedly from outer neritic or uppermost bathyal to a more distinctly (deeper) upper bathyal setting.

## INORGANIC GEOCHEMISTRY

### Interstitial Waters

Interstitial-water samples were taken from the first 10 cores of Hole 813A. Subsequent samples were taken from Cores 133-813A-12H, -15H, -18H, and -21H.

#### *Calcium, Magnesium, and Strontium*

Concentrations of calcium and strontium rise to maximum values of 11.77 mM and 134 $\mu$M, respectively, within the first core of Hole 813A (Table 2 and Fig. 10). Between 4.45 and 107.47 mbsf, concentrations of strontium fall to levels slightly higher than normal seawater values (105 $\mu$M). Below 107.47 mbsf, $Sr^{2+}$ values decrease to concentrations of 99 to 101 $\mu$M. Concentrations of $Ca^2$ also decline below 4.45 mbsf to between 11 and 11.3 mM. At 107.47 mbsf, the $Ca^{2+}$ concentration increases to ~12 mM and remains approximately constant to 193.67 mbsf. Concentrations of $Mg^2$ generally decrease downcore from 51.93 mM at 4.45 mbsf to a minimum of 50.93 mM at 107.47 mbsf. Between 32.17 and 89.17 mbsf, concentrations of $Mg^{2+}$ equals ~52 mM, while farther down the core, concentrations decrease to 51 mM.

The patterns of $Sr^{2+}$, $Ca^{2+}$, and $Mg^{2+}$ concentration are similar at Site 813A. The initial decrease in $Mg^{2+}$, and increase in $Ca^{2+}$ and $Sr^{2+}$, can be attributed to the dissolution of aragonite, which concentration decreases to zero by 30 mbsf, and perhaps to precipitation of a minor amount of dolomite. The increase in $Ca^{2+}$ and the decrease in $Mg^{2+}$ and $Sr^{2+}$ below 107.47 mbsf corresponds to a change in physical properties and lithostratigraphy from Units II to III. The upper unit is marked by a higher water content (70%–60%) compared to the lower unit (60%–50%) (see "Physical Properties" section, this chapter). The boundary between these two units may be marked by a relatively impermeable horizon that has retarded advection and diffusion. It may significant that a low carbonate- and possibly clay-rich horizon was measured between 108 and 114 mbsf coincident with the boundary between Units II and III and the abrupt shift in concentrations of $Sr^{2+}$, $Ca^{2+}$, and $Mg^{2+}$. The position of the break between Units II and III and the separation of the geochemical units corresponds to a major seismic reflector that separates onlapping and prograding sediments (see "Seismic Stratigraphy" section, this chap-

**Table 2. Interstitial water data for Hole 813A.**

| Core, section, interval (cm) | Depth (mbsf) | pH | Alk. (mM) | Sal. (g/kg) | $Cl^-$ (mM) | $Mg^{2+}$ (mM) | $Ca^{2+}$ (mM) | $SO_4^{2-}$ (mM) | P ($\mu$M) | Si ($\mu$M) | $Sr^{2+}$ ($\mu$M) |
|---|---|---|---|---|---|---|---|---|---|---|---|
| Surface seawater: | | 7.99 | 2.455 | 36.2 | 544.84 | 54.46 | 10.46 | 29.89 | 0.58 | 6 | 96 |
| 133-813A | | | | | | | | | | | |
| 1H-3, 145–150 | 4.45 | 7.67 | 3.135 | 35.0 | 544.84 | 51.93 | 11.77 | 30.67 | 0.00 | 82 | 134 |
| 2H-5, 145–150 | 13.17 | 7.34 | 2.927 | 36.0 | 547.72 | 52.66 | 11.45 | 29.24 | 0.85 | 80 | 111 |
| 3H-5, 145–150 | 22.67 | 7.17 | 2.501 | 35.8 | 542.92 | 51.95 | 11.30 | 30.55 | 0.00 | 88 | 107 |
| 4H-5, 145–150 | 32.17 | 7.27 | 2.506 | 35.2 | 540.04 | 51.31 | 11.22 | 28.64 | 0.85 | 66 | 104 |
| 5H-5, 145–150 | 41.67 | 7.16 | 2.679 | 35.5 | 545.80 | 51.82 | 11.18 | 29.38 | 0.00 | 60 | 105 |
| 6H-5, 145–150 | 51.17 | 7.07 | 3.199 | 35.8 | 541.96 | 51.52 | 11.09 | 29.04 | 0.98 | 45 | 104 |
| 7H-5, 145–150 | 60.67 | 7.28 | 2.187 | 35.2 | 541.96 | 51.86 | 11.15 | 29.83 | 0.44 | 39 | 105 |
| 8H-5, 145–150 | 70.17 | 7.30 | 2.200 | 35.2 | 540.04 | 52.06 | 11.26 | 29.47 | 0.71 | 41 | 105 |
| 9H-5, 145–150 | 79.67 | 7.31 | 2.584 | 35.2 | 540.04 | 51.90 | 11.18 | 29.05 | 0.31 | 37 | 105 |
| 10H-5, 145–150 | 89.17 | 7.21 | 2.557 | 35.2 | 542.92 | 51.73 | 11.27 | 29.84 | 0.85 | 39 | 110 |
| 12H-5, 145–150 | 107.47 | 7.43 | 2.767 | 35.2 | 541.96 | 50.99 | 12.10 | 29.91 | 0.58 | 29 | 101 |
| 15H-5, 145–150 | 136.67 | 7.34 | 2.776 | 35.2 | 538.12 | 51.08 | 11.94 | 28.51 | 0.71 | 33 | 99 |
| 18H-5, 145–150 | 165.17 | 7.36 | 2.608 | 35.2 | 542.92 | 51.02 | 11.99 | 29.76 | 0.44 | 43 | 99 |
| 21H-5, 145–150 | 193.67 | 7.62 | 2.755 | 35.2 | 543.88 | 51.15 | 11.86 | 31.20 | 0.58 | 33 | 99 |

Alk. = alkalinity; Sal. = salinity.

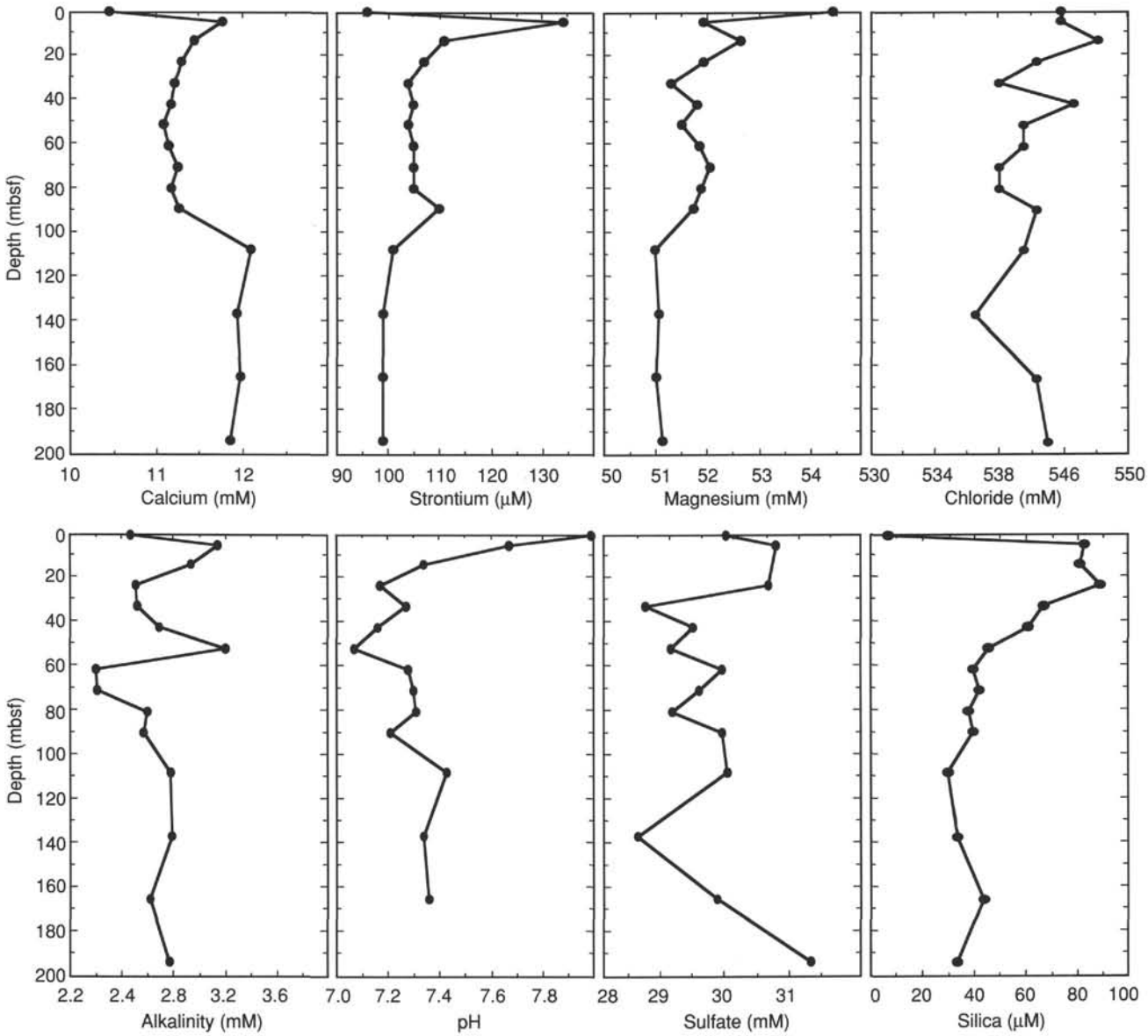


Figure 10. Concentrations of $Ca^{2+}$, $Sr^{2+}$, $Mg^{2+}$, $Cl^-$, alkalinity, pH, $SO_4^{2-}$, and Si as a function of depth in Site 813.

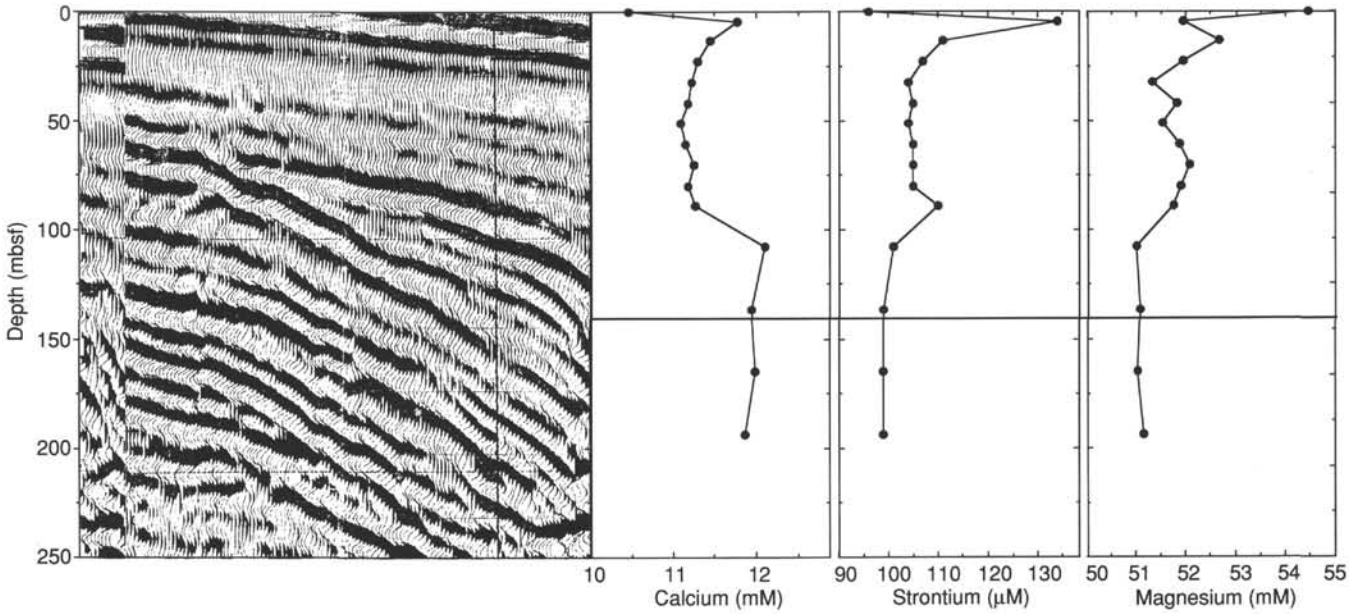


Figure 11. Comparison of the $Ca^{2+}$, $Mg^{2+}$, and $Sr^{2+}$ data with the seismic section for Site 813.

ter). A comparison of the concentrations of $Ca^{2+}$, $Mg^{2+}$, and $Sr^{2+}$ with the major seismic reflectors is shown in Figure 11.

### *Alkalinity, Sulfate, pH, and Phosphate*

The alkalinity at Site 813 shows a variable pattern with increasing depth which cannot be related to other trace or minor element constituents (Fig. 10). This variability is believed to be a consequence of certain analytical problems encountered during the analysis. In particular the datum at 51.17 mbsf is believed to be erroneous. If this point is omitted then there is a gradual decrease in alkalinity with depth, the maximum occurring at 4.45 mbsf. No changes with depth in the concentration of sulfate or phosphate were observed. The apparent absence of sulfate reduction, lack of phosphate, and low alkalinity reflect the low concentration of organic material in the sediments (see "Organic Chemistry" section, this chapter). The relatively high alkalinity value at 4.45 mbsf, which can be correlated with an increase in $Sr^{2+}$ and $Ca^{2+}$, reflects the dissolution of aragonite.

### *Salinity*

The concentration of chloride (between 544.84 and 538.12 mM) remains nearly constant throughout Hole 813A.

### *Silica*

The concentration of silica increases sharply by up to 80 μM between 0 and 13.17 mbsf. Below 20 mbsf, concentrations decrease to between 30 and 40 μM (Fig. 10). The high concentration of silica in Cores 133-813A-1H, -2H, and -3H probably is related to the dissolution of siliceous microfossils in these intervals.

### *Carbonate and X-Ray Diffraction Data*

X-ray diffraction analysis showed that the upper 180 mbsf was dominated by low-Mg calcite (Table 3). Below this depth, dolomite predominates (Fig. 12). Dolomite is also a minor component in the overlying sediments and increases steadily between 40 and 180 mbsf. In the upper 20 mbsf, aragonite formed up to 30% of the carbonate fraction, but this proportion decreases rapidly with depth with the consequence that

**Table 3. Mineralogy from X-ray studies for Hole 813A.**

| Core, section, interval (cm) | Depth (mbsf) | Calcite (%) | Aragonite (%) | Quartz (%) | Dolomite (%) |
|---|---|---|---|---|---|
| 133-813A- | | | | | |
| 1H-2, 77–78 | 2.27 | 63.1 | 31.5 | 4.1 | 1.3 |
| 1H-5, 145–150 | 4.45 | 75.1 | 23.3 | 0.9 | 0.7 |
| 2H-2, 61–62 | 7.80 | 85.0 | 13.9 | 0.0 | 1.1 |
| 2H-5, 145–150 | 13.17 | 81.1 | 18.9 | 0.0 | 0.0 |
| 3H-2, 100–101 | 17.70 | 97.4 | 2.6 | 0.0 | 0.0 |
| 3H-5, 145–150 | 22.67 | 95.6 | 0.0 | 4.4 | 0.0 |
| 4H-2, 100–101 | 27.20 | 97.9 | 0.0 | 0.0 | 2.1 |
| 4H-5, 145–150 | 32.17 | 99.1 | 0.0 | 0.9 | 0.0 |
| 5H-2, 99–100 | 37.70 | 99.0 | 0.0 | 0.0 | 1.0 |
| 5H-5, 145–150 | 41.67 | 99.6 | 0.0 | 0.0 | 0.4 |
| 6H-2, 100–101 | 46.20 | 99.5 | 0.0 | 0.0 | 0.5 |
| 6H-5, 145–150 | 51.17 | 97.2 | 0.0 | 0.0 | 2.8 |
| 7H-1, 60–61 | 53.80 | 93.2 | 0.0 | 4.8 | 1.9 |
| 7H-3, 97–98 | 57.20 | 100.0 | 0.0 | 0.0 | 0.0 |
| 7H-5, 145–150 | 60.67 | 95.8 | 0.0 | 0.0 | 4.2 |
| 8H-2, 71–72 | 64.90 | 97.9 | 0.0 | 0.0 | 2.1 |
| 8H-5, 145–150 | 70.17 | 97.6 | 0.0 | 0.0 | 2.4 |
| 9H-2, 145–150 | 75.00 | 88.9 | 0.0 | 0.0 | 11.1 |
| 9H-5, 145–150 | 79.67 | 88.6 | 0.0 | 0.0 | 11.4 |
| 10H-2, 86–87 | 84.06 | 94.4 | 0.0 | 1.0 | 4.6 |
| 10H-5, 145–150 | 89.17 | 92.2 | 0.0 | 0.0 | 7.8 |
| 11H-2, 90–92 | 93.60 | 94.5 | 0.0 | 0.0 | 5.5 |
| 11H-5, 90–92 | 98.10 | 90.4 | 0.0 | 1.0 | 8.5 |
| 12H-2, 100–102 | 103.20 | 89.3 | 0.0 | 4.3 | 6.3 |
| 12H-5, 145–150 | 107.47 | 94.5 | 0.0 | 0.0 | 5.5 |
| 13H-2, 100–102 | 112.70 | 95.9 | 0.0 | 0.0 | 4.1 |
| 13H-5, 100–102 | 117.70 | 91.7 | 0.0 | 5.3 | 3.0 |
| 14H-2, 102–103 | 122.20 | 95.6 | 0.0 | 0.0 | 4.4 |
| 14H-5, 101–103 | 125.20 | 91.3 | 0.0 | 1.9 | 6.7 |
| 15H-2, 102–103 | 131.70 | 95.1 | 0.0 | 0.0 | 4.9 |
| 16H-2, 102–103 | 141.20 | 92.8 | 0.0 | 0.0 | 7.2 |
| 16H-5, 102–103 | 144.20 | 90.4 | 0.0 | 4.0 | 5.6 |
| 17H-2, 102–103 | 150.70 | 83.9 | 0.0 | 2.8 | 13.3 |
| 17H-5, 102–104 | 153.70 | 88.4 | 0.0 | 1.8 | 9.7 |
| 18H-2, 85–87 | 161.00 | 74.9 | 0.0 | 0.0 | 25.1 |
| 18H-5, 145–150 | 165.17 | 82.1 | 0.0 | 0.0 | 17.9 |
| 19H-2, 40–42 | 169.10 | 80.9 | 0.0 | 0.0 | 19.1 |
| 19H-5, 40–42 | 172.10 | 90.2 | 0.0 | 0.0 | 9.8 |
| 20H-2, 80–82 | 179.00 | 80.5 | 0.0 | 0.0 | 19.5 |
| 20H-5, 80–82 | 182.00 | 85.0 | 0.0 | 2.9 | 12.1 |
| 21H-5, 145–150 | 193.67 | 21.8 | 0.0 | 0.0 | 78.2 |

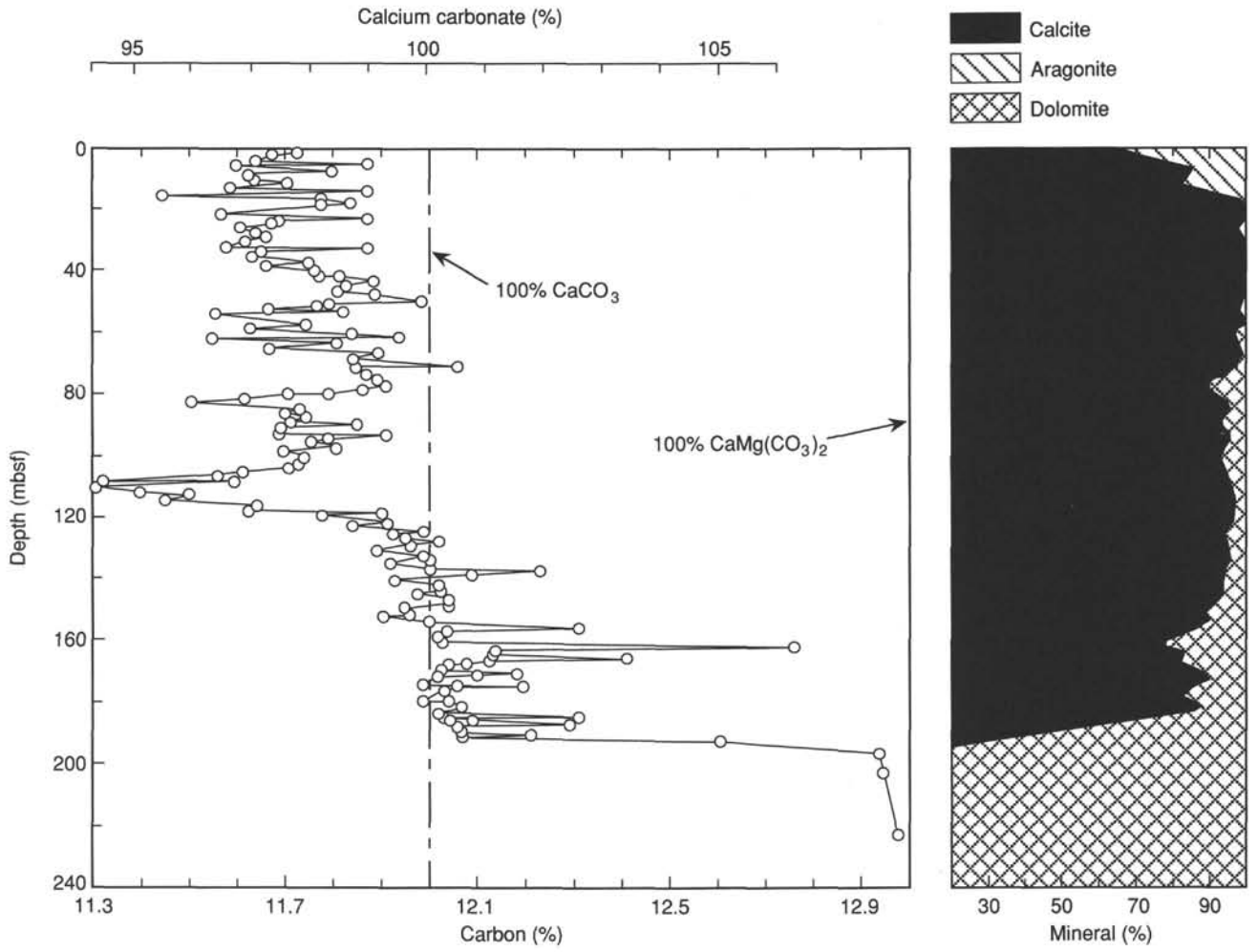


Figure 12. Carbonate content and percentage mineralogy as a function of depth for Site 813. The deepest sample analyzed by XRD from 194.67 mbsf contained 78% dolomite. On the basis of %carbonate and other observations (See "Lithostratigraphy" section, this chapter), 100% dolomite has been indicated to the bottom of the core.

by the Pliocene/Pleistocene contact (22.7 mbsf) aragonite has virtually disappeared.

Carbonate contents are in excess of 95% throughout Hole 813A (Fig. 12 and Table 4). We found that the standard method for reporting inorganic carbon as a percentage of calcium carbonate was inadequate for sediments that contained significant concentrations of dolomite. As dolomite contains approximately 13 wt% carbon, compared to 12 wt% for calcite, samples containing abundant dolomite yielded concentrations of calcium carbonate in excess of 100 wt%. A comparison of data (reported as a percentage of calcium carbonate) and mineralogy is shown in Figure 12. We have not attempted to correct the data regarding percentages of carbonate for the presence of dolomite because we do not have mineralogy data for all samples. However, one can appreciate that the decrease in the percentage of $CaCO_3$ between 40 and 117 mbsf will in fact be significantly greater, taking into account the increase in the percentage of dolomite over the same interval.

## ORGANIC GEOCHEMISTRY

In addition to safety monitoring for hydrocarbons, the main purpose of the shipboard organic geochemistry studies at Site 813 was to assess the amount and type of organic matter preserved in the Pleistocene to middle Miocene sediments of the Queensland Plateau. We determined the total nitrogen, sulfur, carbon, and the organic carbon contents of 23 additional samples collected for chromatographic analyses of the volatile hydrocarbons (headspace samples) using a NA 1500 Carlo Erba NCS analyzer.

### Volatile Hydrocarbons

Light hydrocarbon gases ($C_1$–$C_3$) in sediments were analyzed routinely as part of the safety and pollution-prevention monitoring program, using the headspace technique and the Carle gas chromatograph. The results of 23 analyses from Hole 813A are presented in Table 5.

The sediments at Site 813 contained very low concentrations of hydrocarbon gases. The concentrations of methane in the headspace gas were ~2 ppm, while neither ethane nor propane were detected.

### Organic Carbon Contents

The total organic carbon (TOC) contents recorded in Hole 813A are presented in Table 6. We observed very low to low TOC values in the calcium carbonate-rich or dolomite-rich sediments encountered at Site 813. Most TOC values ranged below 0.40%, and the total nitrogen and sulfur concentrations were below the detection limits of the NCS analyzer. We observed the highest organic contents in four headspace samples with low total inorganic carbon values (Fig. 13): in Sample 133-813A-2H-5, 145–146 cm (TOC = 0.65%, TIC =

**Table 4. Carbonate content data for Hole 813A.**

| Core, section, interval (cm) | Depth (mbsf) | Carbon (wt%) | Carbonate (wt%) |
|---|---|---|---|
| 133-813A | | | |
| 1H-1, 108–110 | 1.08 | 11.62 | 96.8 |
| 1H-2, 77–79 | 2.27 | 11.57 | 96.4 |
| 1H-3, 101–103 | 4.01 | 11.54 | 96.1 |
| 1H-3, 145–146 | 4.45 | 11.77 | 96.7 |
| 1H-4, 72–74 | 5.22 | 11.50 | 95.8 |
| 2H-1, 125–127 | 6.95 | 11.69 | 97.4 |
| 2H-2, 61–63 | 7.81 | 11.52 | 96.0 |
| 2H-3, 99–101 | 9.69 | 11.53 | 96.0 |
| 2H-4, 100–102 | 11.20 | 11.60 | 96.6 |
| 2H-5, 66–68 | 12.36 | 11.49 | 95.7 |
| 2H-5, 145–146 | 13.15 | 11.77 | 92.8 |
| 2H-6, 100–102 | 14.20 | 11.50 | 95.8 |
| 2H-7, 57–59 | 15.27 | 11.35 | 94.5 |
| 3H-1, 98–100 | 16.18 | 11.67 | 97.2 |
| 3H-2, 100–102 | 17.70 | 11.73 | 97.7 |
| 3H-3, 100–102 | 19.20 | 11.67 | 97.2 |
| 3H-4, 100–102 | 20.70 | 11.47 | 95.5 |
| 3H-5, 81–83 | 22.01 | 11.70 | 97.5 |
| 3H-5, 145–146 | 22.65 | 11.77 | 97.0 |
| 3H-6, 103–105 | 23.73 | 11.58 | 96.5 |
| 3H-7, 42–44 | 24.62 | 11.57 | 96.4 |
| 4H-1, 102–104 | 25.72 | 11.51 | 95.9 |
| 4H-2, 100–102 | 27.20 | 11.54 | 96.1 |
| 4H-3, 109–111 | 28.79 | 11.56 | 96.3 |
| 4H-4, 100–102 | 30.20 | 11.52 | 96.0 |
| 4H-5, 101–103 | 31.71 | 11.48 | 95.6 |
| 4H-5, 145–146 | 32.15 | 11.77 | 97.2 |
| 4H-6, 122–124 | 33.42 | 11.55 | 96.2 |
| 5H-1, 101–103 | 35.21 | 11.53 | 96.0 |
| 5H-2, 99–101 | 36.69 | 11.65 | 97.0 |
| 5H-3, 102–104 | 38.22 | 11.56 | 96.3 |
| 5H-4, 101–103 | 39.71 | 11.66 | 97.1 |
| 5H-5, 99–101 | 41.19 | 11.71 | 97.5 |
| 5H-5, 145–146 | 41.65 | 11.67 | 97.0 |
| 5H-6, 101–103 | 42.71 | 11.78 | 98.1 |
| 6H-1, 98–100 | 44.68 | 11.72 | 97.6 |
| 6H-2, 100–102 | 46.20 | 11.71 | 97.5 |
| 6H-3, 97–99 | 47.67 | 11.79 | 98.2 |
| 6H-4, 101–103 | 49.21 | 11.89 | 99.0 |
| 6H-5, 101–102 | 50.71 | 11.70 | 97.5 |
| 6H-5, 145–146 | 51.15 | 11.67 | 96.8 |
| 6H-6, 100–102 | 52.20 | 11.57 | 96.4 |
| 6H-7, 53–56 | 53.23 | 11.72 | 97.6 |
| 7H-1, 60–63 | 53.80 | 11.46 | 95.5 |
| 7H-3, 97–100 | 57.17 | 11.64 | 97.0 |
| 7H-4, 97–100 | 58.67 | 11.53 | 96.0 |
| 7H-5, 97–100 | 60.17 | 11.74 | 97.8 |
| 7H-5, 145–146 | 60.65 | 11.83 | 98.0 |
| 7H-6, 97–100 | 61.67 | 11.45 | 95.4 |
| 7H-7, 77–81 | 62.97 | 11.70 | 97.5 |
| 8H-1, 71–74 | 63.41 | 11.63 | 96.9 |
| 8H-2, 71–74 | 64.91 | 11.57 | 96.4 |
| 8H-3, 71–74 | 66.41 | 11.79 | 98.2 |
| 8H-4, 71–74 | 67.91 | 11.74 | 97.8 |
| 8H-5, 71–74 | 69.41 | 11.77 | 98.0 |
| 8H-5, 145–146 | 70.15 | 11.96 | 98.5 |
| 8H-6, 71–74 | 70.91 | 11.75 | 97.9 |
| 9H-1, 140–143 | 73.60 | 11.77 | 98.0 |
| 9H-2, 140–143 | 75.10 | 11.80 | 98.3 |
| 9H-3, 140–143 | 76.60 | 11.81 | 98.4 |
| 9H-4, 140–143 | 78.10 | 11.76 | 98.0 |
| 9H-5, 113–116 | 79.33 | 11.69 | 97.4 |
| 9H-5, 145–146 | 79.65 | 11.61 | 95.1 |
| 9H-6, 140–143 | 81.10 | 11.51 | 95.9 |
| 10H-1, 86–89 | 82.56 | 11.41 | 95.0 |
| 10H-2, 86–89 | 84.06 | 11.63 | 96.9 |
| 10H-3, 86–89 | 85.56 | 11.60 | 96.6 |
| 10H-4, 86–89 | 87.06 | 11.64 | 97.0 |
| 10H-5, 90–93 | 88.60 | 11.62 | 96.8 |
| 10H-5, 145–146 | 89.15 | 11.75 | 93.5 |
| 10H-6, 90–93 | 90.10 | 11.59 | 96.5 |
| 11H-1, 90–93 | 92.10 | 11.59 | 96.5 |
| 11H-1, 149–150 | 92.69 | 11.81 | 96.7 |
| 11H-2, 90–93 | 93.60 | 11.69 | 97.4 |
| 11H-3, 90–93 | 95.10 | 11.65 | 97.0 |
| 11H-4, 90–93 | 96.60 | 11.71 | 97.5 |

**Table 4 (continued).**

| Core, section, interval (cm) | Depth (mbsf) | Carbon (wt%) | Carbonate (wt%) |
|---|---|---|---|
| 11H-5, 90–93 | 98.10 | 11.60 | 96.6 |
| 11H-6, 90–93 | 99.60 | 11.64 | 97.0 |
| 12H-1, 100–103 | 101.70 | 11.63 | 96.9 |
| 12H-2, 100–103 | 103.20 | 11.61 | 96.7 |
| 12H-3, 100–103 | 104.70 | 11.51 | 95.9 |
| 12H-4, 100–103 | 106.20 | 11.46 | 95.5 |
| 12H-5, 96–99 | 107.66 | 11.23 | 93.5 |
| 12H-5, 145–146 | 108.15 | 11.49 | 92.6 |
| 12H-6, 96–99 | 109.16 | 11.21 | 93.4 |
| 13H-1, 100–103 | 111.20 | 11.30 | 94.1 |
| 13H-2, 100–103 | 112.70 | 11.40 | 95.0 |
| 13H-3, 100–103 | 114.20 | 11.36 | 94.6 |
| 13H-4, 100–103 | 115.70 | 11.54 | 96.1 |
| 13H-5, 100–103 | 117.20 | 11.53 | 96.0 |
| 13H-5, 149–150 | 117.69 | 11.80 | 96.7 |
| 13H-6, 100–103 | 118.70 | 11.68 | 97.3 |
| 14H-1, 101–104 | 120.71 | 11.81 | 98.4 |
| 14H-2, 102–104 | 122.22 | 11.75 | 97.9 |
| 14H-3, 101–104 | 123.71 | 11.88 | 99.0 |
| 14H-4, 101–104 | 125.21 | 11.83 | 98.5 |
| 14H-5, 101–104 | 126.71 | 11.85 | 98.7 |
| 14H-5, 149–150 | 127.19 | 11.92 | 98.2 |
| 14H-6, 101–104 | 128.21 | 11.86 | 98.8 |
| 15H-1, 102–104 | 130.22 | 11.79 | 98.2 |
| 15H-2, 102–104 | 131.72 | 11.88 | 99.0 |
| 15H-3, 102–104 | 133.22 | 11.90 | 99.1 |
| 15H-4, 102–104 | 134.72 | 11.82 | 98.5 |
| 15H-5, 92–94 | 136.12 | 11.90 | 99.1 |
| 15H-5, 145–146 | 136.65 | 12.13 | 100.4 |
| 15H-6, 101–103 | 137.71 | 11.99 | 99.9 |
| 16H-1, 108–110 | 139.78 | 11.83 | 98.5 |
| 16H-2, 102–104 | 141.22 | 11.92 | 99.3 |
| 16H-3, 102–104 | 142.72 | 11.92 | 99.3 |
| 16H-4, 102–104 | 144.22 | 11.88 | 99.0 |
| 16H-5, 102–104 | 145.72 | 11.94 | 99.5 |
| 16H-6, 102–104 | 147.22 | 11.94 | 99.5 |
| 17H-1, 102–104 | 149.22 | 11.85 | 98.7 |
| 17H-2, 102–104 | 150.72 | 11.86 | 98.8 |
| 17H-3, 102–104 | 152.22 | 11.81 | 98.4 |
| 17H-4, 102–104 | 153.72 | 11.90 | 99.1 |
| 17H-5, 102–104 | 155.22 | 11.97 | 99.7 |
| 17H-5, 149–150 | 155.69 | 12.21 | 97.5 |
| 17H-6, 102–104 | 156.72 | 11.94 | 99.5 |
| 18H-1, 85–86 | 158.55 | 11.92 | 99.3 |
| 18H-2, 85–86 | 160.05 | 11.93 | 99.4 |
| 18H-3, 85–86 | 161.55 | 12.66 | 105.5 |
| 18H-4, 85–86 | 163.05 | 12.04 | 100.3 |
| 18H-5, 85–86 | 164.55 | 12.03 | 100.2 |
| 18H-5, 149–150 | 165.19 | 12.31 | 99.9 |
| 18H-6, 85–86 | 166.05 | 12.03 | 100.2 |
| 18H-7, 60–63 | 167.30 | 11.98 | 99.8 |
| 19H-1, 40–43 | 167.60 | 11.94 | 99.5 |
| 19H-2, 40–43 | 169.10 | 11.93 | 99.4 |
| 19H-3, 40–43 | 170.60 | 12.08 | 100.6 |
| 19H-4, 40–43 | 172.10 | 11.91 | 99.2 |
| 19H-5, 40–43 | 173.60 | 11.89 | 99.0 |
| 19H-5, 149–150 | 174.69 | 12.10 | 99.4 |
| 19H-6, 40–43 | 175.10 | 11.96 | 99.6 |
| 19H-7, 40–43 | 176.60 | 11.91 | 99.2 |
| 20H-1, 80–83 | 177.50 | 11.93 | 99.4 |
| 20H-2, 80–83 | 179.00 | 11.89 | 99.0 |
| 20H-3, 80–83 | 180.50 | 11.95 | 99.5 |
| 20H-4, 80–83 | 182.00 | 11.97 | 99.7 |
| 20H-5, 80–83 | 183.50 | 11.92 | 99.3 |
| 20H-5, 149–150 | 184.19 | 12.21 | 99.2 |
| 20H-6, 80–83 | 185.00 | 11.93 | 99.4 |
| 21H-1, 4–7 | 186.24 | 12.02 | 100.1 |
| 20H-7, 65–67 | 186.35 | 11.95 | 99.5 |
| 21H-2, 4–7 | 186.84 | 12.19 | 101.5 |
| 21H-3, 25–28 | 187.89 | 11.97 | 99.7 |
| 21H-4, 25–28 | 189.39 | 11.97 | 99.7 |
| 21H-4, 145–146 | 190.59 | 12.11 | 100.2 |
| 21H-5, 27–31 | 190.91 | 11.97 | 99.7 |
| 21H-6, 32–35 | 192.46 | 12.51 | 104.2 |
| 22H-1, 0–2 | 195.70 | 12.84 | 104.5 |
| 23H-1, 0–2 | 202.4 | 12.85 | 105.5 |
| 26H-1, 0–2 | 222.1 | 12.88 | 105.5 |

**Table 5. Volatile hydrocarbon data from headspace analysis at Hole 813A.**

| Core, section, interval (cm) | Depth (mbsf) | Sample type | Volume (mL) | Gas chromato. | $C_1$ (ppm) | $C_{2+}$ (ppm) |
|---|---|---|---|---|---|---|
| 133-813A- | | | | | | |
| 1H-3, 145–146 | 4.45 | HS | 5 | CAR132 | 2 | 0 |
| 2H-5, 145–146 | 13.15 | HS | 5 | CAR132 | 2 | 0 |
| 3H-5, 145–146 | 22.65 | HS | 5 | CAR132 | 2 | 0 |
| 4H-5, 145–146 | 32.15 | HS | 5 | CAR132 | 2 | 0 |
| 5H-5, 145–146 | 41.65 | HS | 5 | CAR132 | 2 | 0 |
| 6H-5, 145–146 | 51.15 | HS | 5 | CAR132 | 2 | 0 |
| 7H-5, 145–146 | 60.65 | HS | 5 | CAR132 | 2 | 0 |
| 8H-5, 145–146 | 70.15 | HS | 5 | CAR132 | 2 | 0 |
| 9H-5, 145–146 | 79.65 | HS | 5 | CAR132 | 2 | 0 |
| 10H-5, 145–146 | 89.15 | HS | 5 | CAR132 | 2 | 0 |
| 11H-1, 149–150 | 92.69 | HS | 5 | CAR132 | 2 | 0 |
| 12H-5, 145–146 | 108.15 | HS | 5 | CAR132 | 2 | 0 |
| 13H-5, 149–150 | 117.69 | HS | 5 | CAR132 | 2 | 0 |
| 14H-5, 149–150 | 127.19 | HS | 5 | CAR132 | 2 | 0 |
| 15H-5, 149–150 | 136.69 | HS | 5 | CAR132 | 2 | 0 |
| 17H-5, 149–150 | 155.69 | HS | 5 | CAR132 | 2 | 0 |
| 18H-5, 149–150 | 165.19 | HS | 5 | CAR132 | 2 | 0 |
| 19H-5, 149–150 | 174.69 | HS | 5 | CAR132 | 2 | 0 |
| 20H-5, 149–150 | 184.19 | HS | 5 | CAR132 | 2 | 0 |
| 21H-4, 145–146 | 190.59 | HS | 5 | CAR132 | 2 | 0 |
| 22X-1, 0–2 | 195.7 | HS | 5 | CAR132 | 2 | 0 |
| 23X-CC, 0–2 | 202.4 | HS | 5 | CAR132 | 2 | 0 |
| 26X-CC, 0–2 | 222.1 | HS | 5 | CAR132 | 2 | 0 |

HS = headspace sample.

**Table 6. Concentrations of total organic carbon, inorganic carbon, and carbon in sediments at Hole 813A.**

| Core, section, interval (cm) | Depth (mbsf) | Sample type | Total organic carbon (%) | Inorganic carbon (%) | Total carbon (%) |
|---|---|---|---|---|---|
| 133-813A- | | | | | |
| 1H-3, 145–146 | 4.45 | HS | 0.15 | 11.6 | 11.75 |
| 2H-5, 145–146 | 13.15 | HS | 0.65 | 11.15 | 11.8 |
| 3H-5, 145–146 | 22.65 | HS | 0.1 | 11.65 | 11.75 |
| 4H-5, 145–146 | 32.15 | HS | 0.1 | 11.65 | 11.75 |
| 5H-5, 145–146 | 41.65 | HS | 0.05 | 11.65 | 11.7 |
| 6H-5, 145–146 | 51.15 | HS | 0.05 | 11.6 | 11.65 |
| 7H-5, 145–146 | 60.65 | HS | 0.05 | 11.75 | 11.8 |
| 8H-5, 145–146 | 70.15 | HS | 0.15 | 11.85 | 12 |
| 9H-5, 145–146 | 79.65 | HS | 0.2 | 11.4 | 11.6 |
| 10H-5, 145–146 | 89.15 | HS | 0.5 | 11.25 | 11.75 |
| 11H-1, 149–150 | 92.69 | HS | 0.2 | 11.6 | 11.8 |
| 12H-5, 145–146 | 108.15 | HS | 0.4 | 11.1 | 11.5 |
| 13H-5, 149–150 | 117.69 | HS | 0.2 | 11.6 | 11.8 |
| 14H-5, 149–150 | 127.19 | HS | 0.1 | 11.8 | 11.9 |
| 15H-5, 145–146 | 136.65 | HS | 0.1 | 12.05 | 12.15 |
| 17H-5, 149–150 | 155.69 | HS | 0.5 | 11.7 | 12.2 |
| 18H-5, 149–150 | 165.19 | HS | 0.3 | 12 | 12.3 |
| 19H-5, 149–150 | 174.69 | HS | 0.2 | 11.9 | 12.1 |
| 20H-5, 149–150 | 184.19 | HS | 0.3 | 11.9 | 12.2 |
| 21H-4, 145–146 | 190.59 | HS | 0.1 | 12 | 12.1 |
| 22X-1, 0–2 | 195.7 | HS | 0.3 | 12.55 | 12.85 |
| 23X-CC, 0–2 | 202.4 | HS | 0.2 | 12.65 | 12.85 |
| 26X-CC, 0–2 | 222.1 | HS | 0.2 | 12.7 | 12.9 |

HS = headspace.

11.15%); in Sample 133-813A-10-H5, 145–146 cm (TOC = 0.5%, TIC = 11.25%); in Sample 133-813A-12H-5, 145–146 cm (TOC = 0.4%, TIC = 11.10%); and in Sample 133-813A-17H-5, 149–150 cm (TOC = 0.5%, TIC = 11.70%). The small increase in TOC content may be the result of a better preservation of organic matter in the clay-richer sediments at Site 813. However, as a consequence of the low organic contents, we were unable to conduct detailed geochemical characterization of kerogen types using the Rock-Eval pyrolysis method, as originally planned.

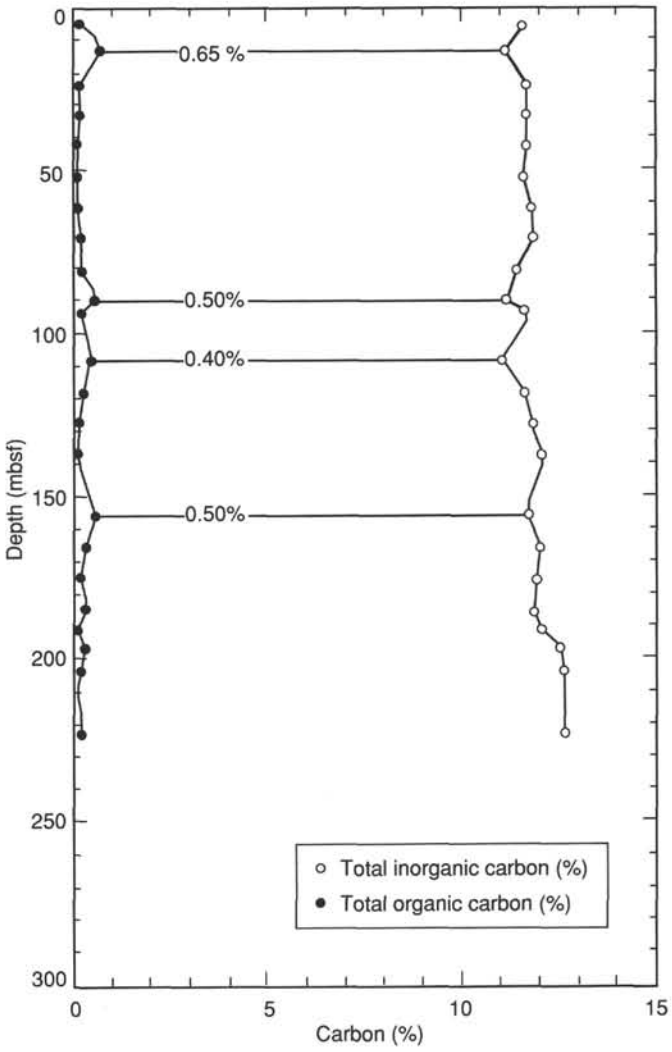


Figure 13. Total organic carbon and total inorganic carbon contents of sediments at Site 813.

## PHYSICAL PROPERTIES

Physical properties analyzed in cores from this site include bulk density, P-wave velocity, and magnetic susceptibility on unsplit cores and P-wave velocity, electrical resistivity formation factor, shear strength, and index properties (including bulk density, grain density, water content, porosity, and void ratio) on split cores. The methods used are described in detail in the "Explanatory Notes" chapter of this volume.

### Bulk Density

Bulk density shows a first order trend increasing downward with a 40-m-thick interval having low-density values centered at about 90 mbsf (see Table 7; Figs. 14 and 15). The densities determined using the GRAPE and the pycnometer show the same overall pattern with similar amounts of scatter.

### *P*-Wave Velocity

*P*-wave velocities indicate the same pattern as densities, with a 40-m-thick interval having low velocity values centered on about 90 mbsf (see Table 8; Figs. 14 and 15).

**Table 7. Index properties data at Hole 813A.**

| Core, section, interval (cm) | Depth (mbsf) | Bulk density ($g/cm^3$) | Grain density ($g/cm^3$) | Porosity (%) | Water content (%) | Void ratio |
|---|---|---|---|---|---|---|
| 133-813A- | | | | | | |
| 1H-1, 105–108 | 1.05 | 1.75 | 2.72 | 67 | 64 | 1.99 |
| 1H-2, 76–79 | 2.26 | 1.57 | 2.87 | 61 | 67 | 1.58 |
| 1H-3, 101–104 | 4.01 | 1.87 | 2.91 | 69 | 60 | 2.18 |
| 1H-4, 71–74 | 5.21 | 1.75 | 2.88 | 65 | 61 | 1.84 |
| 2H-2, 81–84 | 8.01 | 1.73 | 2.81 | 71 | 72 | 2.45 |
| 2H-3, 101–104 | 9.71 | 1.80 | 2.87 | 69 | 65 | 2.23 |
| 2H-5, 66–69 | 12.36 | 1.78 | 2.62 | 67 | 63 | 2.04 |
| 2H-6, 101–104 | 14.21 | 1.87 | 2.91 | 69 | 61 | 2.26 |
| 3H-2, 101–104 | 17.71 | 1.77 | 2.68 | 68 | 65 | 2.14 |
| 3H-3, 101–104 | 19.21 | 1.69 | 2.75 | 66 | 66 | 1.90 |
| 3H-4, 101–104 | 20.71 | 1.81 | 2.86 | 67 | 61 | 2.04 |
| 3H-5, 71–74 | 21.91 | 1.82 | 2.52 | 69 | 63 | 2.18 |
| 3H-6, 101–104 | 23.71 | 1.79 | 2.65 | 71 | 68 | 2.42 |
| 3H-7, 41–44 | 24.61 | 1.88 | 2.84 | 72 | 65 | 2.57 |
| 4H-1, 111–114 | 25.81 | 1.78 | 2.68 | 69 | 66 | 2.27 |
| 4H-2, 101–104 | 27.21 | 1.84 | 2.76 | 68 | 61 | 2.13 |
| 4H-3, 111–114 | 28.81 | 1.99 | 2.68 | 69 | 55 | 2.18 |
| 4H-4, 101–104 | 30.21 | 1.85 | 2.64 | 69 | 61 | 2.19 |
| 4H-5, 101–104 | 31.71 | 1.85 | 2.92 | 70 | 63 | 2.34 |
| 5H-1, 101–104 | 35.21 | 1.98 | 2.72 | 68 | 54 | 2.09 |
| 5H-2, 101–104 | 36.71 | 1.86 | 2.90 | 67 | 58 | 1.99 |
| 5H-3, 101–104 | 38.21 | 1.80 | 2.57 | 66 | 61 | 1.96 |
| 5H-4, 101–104 | 39.71 | 1.95 | 2.87 | 65 | 52 | 1.85 |
| 5H-6, 101–104 | 42.71 | 1.69 | 2.77 | 60 | 58 | 1.52 |
| 6H-1, 101–104 | 44.71 | 1.84 | 2.79 | 64 | 56 | 1.80 |
| 6H-2, 101–104 | 46.21 | 1.97 | 2.54 | 68 | 55 | 2.14 |
| 6H-4, 101–104 | 49.21 | 1.90 | 2.73 | 62 | 50 | 1.61 |
| 6H-5, 101–104 | 50.71 | 1.90 | 2.67 | 64 | 53 | 1.78 |
| 6H-6, 101–104 | 52.21 | 1.84 | 2.83 | 65 | 57 | 1.87 |
| 6H-7, 52–55 | 53.22 | 1.61 | 2.71 | 56 | 55 | 1.27 |
| 7H-1, 60–63 | 53.80 | 1.86 | 2.66 | 71 | 65 | 2.47 |
| 7H-3, 96–99 | 57.16 | 1.80 | 2.79 | 67 | 61 | 1.99 |
| 7H-4, 97–100 | 58.67 | 1.81 | 2.77 | 63 | 55 | 1.69 |
| 7H-6, 97–100 | 61.67 | 1.86 | 2.74 | 62 | 52 | 1.62 |
| 7H-7, 77–80 | 62.97 | 1.89 | 2.70 | 63 | 52 | 1.68 |
| 8H-1, 70–73 | 63.40 | 1.96 | 2.85 | 59 | 45 | 1.45 |
| 8H-2, 70–73 | 64.90 | 1.72 | 2.50 | 63 | 59 | 1.67 |
| 8H-3, 70–73 | 66.40 | 1.72 | 2.70 | 62 | 59 | 1.63 |
| 8H-4, 70–73 | 67.90 | 1.77 | 2.20 | 64 | 59 | 1.79 |
| 8H-5, 70–73 | 69.40 | 1.76 | 2.76 | 63 | 58 | 1.67 |
| 8H-6, 70–73 | 70.90 | 1.75 | 2.78 | 63 | 58 | 1.68 |
| 9H-1, 140–143 | 73.60 | 1.77 | 2.74 | 62 | 56 | 1.64 |
| 9H-2, 140–143 | 75.10 | 1.85 | 2.92 | 61 | 50 | 1.54 |
| 9H-3, 140–143 | 76.60 | 1.75 | 2.83 | 63 | 58 | 1.71 |
| 9H-4, 140–143 | 78.10 | 1.71 | 2.78 | 66 | 66 | 1.95 |
| 9H-5, 140–143 | 79.60 | 1.75 | 2.83 | 69 | 68 | 2.23 |
| 9H-6, 140–143 | 81.10 | 1.75 | 2.80 | 71 | 70 | 2.39 |
| 10H-1, 86–89 | 82.56 | 1.83 | 2.97 | 78 | 77 | 3.44 |
| 10H-2, 86–89 | 84.06 | 1.74 | 2.83 | 71 | 72 | 2.43 |
| 10H-3, 86–89 | 85.56 | 1.74 | 2.54 | 67 | 65 | 2.04 |
| 10H-4, 86–89 | 87.06 | 1.81 | 2.89 | 70 | 66 | 2.38 |
| 10H-5, 90–93 | 88.60 | 1.78 | 2.82 | 66 | 61 | 1.94 |
| 10H-6, 90–93 | 90.10 | 1.79 | 2.67 | 70 | 67 | 2.31 |
| 11H-1, 90–93 | 92.10 | 1.72 | 2.60 | 70 | 71 | 2.33 |
| 11H-2, 90–93 | 93.60 | 1.80 | 2.72 | 69 | 65 | 2.26 |
| 11H-3, 90–93 | 95.10 | 1.72 | 2.91 | 67 | 67 | 2.06 |
| 11H-4, 90–93 | 96.60 | 1.76 | 2.75 | 70 | 69 | 2.33 |

**Table 7 (continued).**

| Core, section, interval (cm) | Depth (mbsf) | Bulk density ($g/cm^3$) | Grain density ($g/cm^3$) | Porosity (%) | Water content (%) | Void ratio |
|---|---|---|---|---|---|---|
| 11H-5, 90–93 | 98.10 | 1.68 | 2.60 | 73 | 80 | 2.66 |
| 11H-6, 90–93 | 99.60 | 1.78 | 2.55 | 65 | 59 | 1.83 |
| 12H-1, 100–103 | 101.70 | 1.73 | 2.85 | 66 | 64 | 1.93 |
| 12H-2, 100–103 | 103.20 | 1.83 | 2.76 | 66 | 59 | 1.96 |
| 12H-4, 100–103 | 106.20 | 1.86 | 2.56 | 65 | 56 | 1.86 |
| 12H-5, 100–103 | 107.70 | 1.84 | 2.92 | 64 | 56 | 1.81 |
| 12H-6, 100–103 | 109.20 | 1.91 | 2.65 | 64 | 52 | 1.74 |
| 13H-1, 100–103 | 111.20 | 1.86 | 2.84 | 72 | 65 | 2.54 |
| 13H-2, 100–103 | 112.70 | 1.78 | 2.89 | 66 | 61 | 1.91 |
| 13H-3, 100–103 | 114.20 | 2.26 | 2.51 | 81 | 58 | 4.22 |
| 13H-4, 100–103 | 115.70 | 2.15 | 2.74 | 72 | 52 | 2.55 |
| 13H-6, 100–103 | 118.70 | 1.61 | 2.68 | 56 | 56 | 1.28 |
| 14H-1, 101–104 | 120.71 | 1.92 | 2.78 | 63 | 50 | 1.68 |
| 14H-2, 101–104 | 122.21 | 1.85 | 2.70 | 62 | 52 | 1.63 |
| 14H-3, 101–104 | 123.71 | 2.05 | 2.58 | 56 | 39 | 1.27 |
| 14H-4, 101–104 | 125.21 | 1.94 | 2.69 | 59 | 45 | 1.44 |
| 14H-5, 101–104 | 126.71 | 2.20 | 2.91 | 71 | 50 | 2.49 |
| 14H-6, 101–104 | 128.21 | 1.68 | 2.64 | 49 | 42 | 0.94 |
| 15H-1, 101–104 | 130.21 | 1.88 | 2.51 | 61 | 50 | 1.54 |
| 15H-2, 101–104 | 131.71 | 1.97 | 2.75 | 59 | 44 | 1.43 |
| 15H-3, 101–104 | 133.21 | 2.02 | 2.87 | 56 | 39 | 1.25 |
| 15H-4, 101–104 | 134.71 | 1.97 | 2.92 | 56 | 42 | 1.29 |
| 15H-5, 91–93 | 136.11 | 1.82 | 2.60 | 54 | 44 | 1.18 |
| 15H-6, 101–104 | 137.71 | 2.10 | 2.77 | 51 | 33 | 1.06 |
| 16H-1, 101–104 | 139.71 | 2.26 | 2.66 | 67 | 44 | 2.06 |
| 16H-2, 101–104 | 141.21 | 2.02 | 2.83 | 59 | 42 | 1.42 |
| 16H-5, 101–104 | 145.71 | 1.98 | 2.88 | 55 | 39 | 1.20 |
| 17H-1, 101–104 | 149.21 | 1.96 | 2.83 | 56 | 42 | 1.28 |
| 17H-2, 101–104 | 150.71 | 1.89 | 2.59 | 57 | 44 | 1.30 |
| 17H-3, 101–104 | 152.21 | 1.88 | 2.71 | 53 | 40 | 1.11 |
| 17H-4, 101–104 | 153.71 | 2.01 | 2.91 | 53 | 37 | 1.12 |
| 17H-5, 101–104 | 155.21 | 2.16 | 2.79 | 56 | 36 | 1.27 |
| 17H-6, 101–104 | 156.71 | 2.01 | 2.66 | 59 | 43 | 1.41 |
| 18H-1, 80–83 | 158.50 | 2.12 | 2.65 | 65 | 46 | 1.85 |
| 18H-2, 80–83 | 160.00 | 2.10 | 2.84 | 56 | 38 | 1.28 |
| 18H-4, 80–83 | 163.00 | 2.02 | 2.67 | 50 | 34 | 0.99 |
| 18H-5, 80–83 | 164.50 | 2.09 | 2.75 | 56 | 37 | 1.25 |
| 18H-6, 80–83 | 166.00 | 1.93 | 2.77 | 53 | 39 | 1.13 |
| 18H-7, 60–63 | 167.30 | 2.10 | 2.92 | 53 | 35 | 1.12 |
| 19H-2, 80–83 | 169.50 | 2.08 | 2.81 | 53 | 36 | 1.14 |
| 19H-3, 80–83 | 171.00 | 2.13 | 2.71 | 50 | 31 | 0.99 |
| 19H-4, 80–83 | 172.50 | 2.04 | 2.74 | 52 | 35 | 1.08 |
| 19H-5, 80–83 | 174.00 | 1.99 | 2.79 | 54 | 38 | 1.17 |
| 19H-6, 80–83 | 175.50 | 2.08 | 2.74 | 49 | 32 | 0.97 |
| 19H-7, 60–63 | 176.80 | 2.15 | 2.64 | 44 | 27 | 0.79 |
| 20H-1, 80–83 | 177.50 | 2.04 | 2.76 | 51 | 34 | 1.04 |
| 20H-2, 80–83 | 179.00 | 1.91 | 2.65 | 52 | 39 | 1.08 |
| 20H-3, 80–83 | 180.50 | 2.02 | 2.70 | 51 | 34 | 1.02 |
| 20H-4, 80–83 | 182.00 | 2.01 | 2.66 | 49 | 33 | 0.96 |
| 20H-5, 80–83 | 183.50 | 2.04 | 2.76 | 48 | 31 | 0.90 |
| 20H-6, 80–83 | 185.00 | 1.98 | 2.81 | 51 | 36 | 1.05 |
| 21H-1, 4–7 | 186.24 | 2.02 | 2.80 | 48 | 33 | 0.94 |
| 20H-7, 60–63 | 186.30 | 2.11 | 2.58 | 49 | 32 | 0.97 |
| 21H-2, 4–7 | 186.84 | 2.10 | 2.76 | 49 | 31 | 0.95 |
| 21H-3, 30–33 | 187.94 | 2.06 | 2.94 | 53 | 36 | 1.14 |
| 21H-4, 25–28 | 189.39 | 2.04 | 2.84 | 45 | 29 | 0.83 |
| 21H-5, 28–31 | 190.92 | 2.00 | 2.87 | 52 | 37 | 1.10 |
| 21H-6, 32–35 | 192.46 | 2.05 | 2.85 | 49 | 32 | 0.95 |

## Porosity and Dry-Water Content

Porosity was one of the index properties determined from the pycnometer measurements. A graph of porosity vs. depth is shown in Figure 15. Similarly, the dry-water content, which is calculated from the same volume and weight measurements as porosity, also has been plotted in Figure 15. Both show a general decrease with depth, with a 40-m-thick interval of high porosity and water content values centered at about 90 mbsf.

## Electrical-Resistivity Formation Factor

We measured the formation factor (FF) at three intervals in each section from Hole 813A (see Table 9 and Fig. 15). Despite large scatter among closely spaced measurements, FF data show broad trends similar to those seen in dry-water content, shear strength, and sonic velocity. Two regions of high FF values are centered at 50 and 150 mbsf, respectively, suggesting that we measured a real geologic signal.

## Shear Strength

The shear strength showed a great deal of variability, although most values ranged from 1 to 10 kPa (see Table 10 and Fig. 15). The great variability between adjacent points may not represent real variability of the shear strength of the section; however, the generally low shear strength between 75 and 125 m in the hole corresponds to lows in the formation

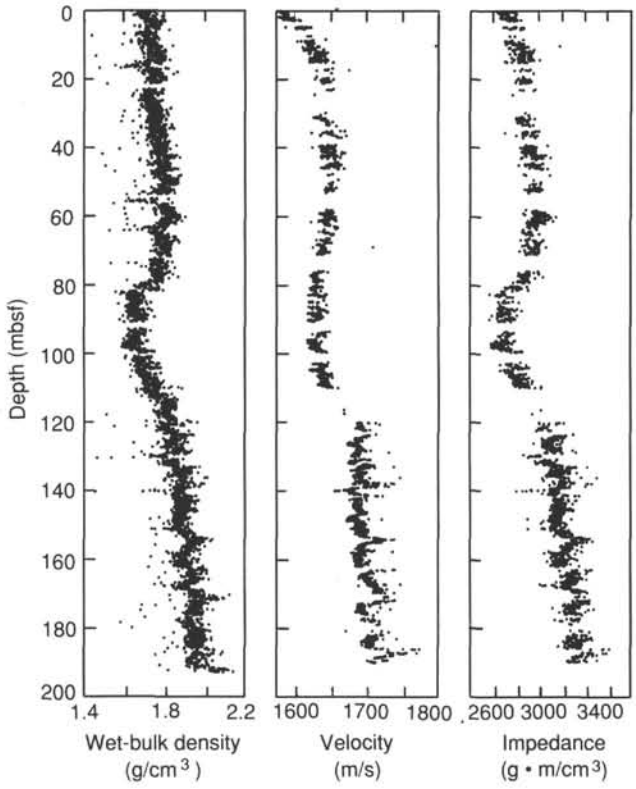


Figure 14. Comparison of MST sonic velocity with GRAPE density for Hole 813A. The data points on this figure are produced by averaging all data in 5-cm-long blocks from both the GRAPE and MST velocity data files. The impedance was calculated by multiplying the GRAPE density values by the MST velocity values.

factor, bulk density, and sonic velocity, and a high in the dry-water content, suggesting that the broad trends in shear strength are representative of the section.

## SEISMIC STRATIGRAPHY

The seismic stratigraphic interpretation for Site 813, comparing the stratigraphic and the sedimentological data, is outlined below. The time-depth velocity plot shown in Figure 4 was calculated during the cruise in order to compare the seismic data with the drilling results and to predict lithologies ahead of the drilling.

An east-west line (Fig. 16A) connects Sites 813 and 814 and will be used in both site descriptions. Our interpretation of the seismic stratigraphy at Site 813 is shown in Figure 16B.

At Site 813, five seismic reflectors have been identified as unconformities separating six seismic sequences.

Seismic sequence 1 occurs between the seafloor and reflector 1 at 760 ms. It is approximately 60 ms thick at the drill site, but thickens to the west. Onlap to the east is visible. Reflector 1 is an unconformity, which on the basis of a comparison with the dated depths of the core, may correspond with a late Pliocene lowstand and transgression at about 2.4 Ma. Sequence 1 equates with the upper part of lithologic Unit I, described as a micritic foraminifer ooze with nannofossils and bioclasts which contains some chalkification. It is considered to have been deposited in an upper bathyal environment. It is clear that the unconformity at the base of the sequence corresponding with the 2.42 Ma lowstand and the transgressive onlap are not seen in the lithostratigraphic data, suggesting that the environment changed little in spite of the 2.4 Ma globally recorded regression and transgression. The onlap seen above reflector 1 defines a shift in the depositional locus, but apparently no change in sediment type. To this extent the seismic data is both important and misleading.

Sequence 2 occurs between reflectors 2 and 3 and is 30 ms thick at the drill site, becoming increasingly thicker westward and thinning eastward. Onlap is clearly visible within the sequence suggesting deposition during a rising sea level. The base of sequence 2 is proposed to correspond with an early Pliocene lowstand at 3.0 Ma, which equates with the bottom of lithostratigraphic Unit I. Onlap is seen against the basal reflector. If the above correlations are correct, then sequence 2 may be defined as a foraminifer-nannofossil ooze with bioclasts and some micrite deposited in an upper bathyal environment. If the lower boundary of Unit I is truly 3.0 Ma, then the time period for the deposition of sequence 2 is 3.0–2.4 Ma, much of which was a low-sea-level period. The basal sequence boundary thus should define a condensed sequence; However, this was not seen in the lithologic unit. Deposition within sequence 2 (= lower part of lithologic Unit I) thusshould have occurred within the two short highstands at 2.7 and 2.5 Ma. However, the lithologies indicate little change, suggesting either that the correlations are wrong or that the proposed shifts in sea level were not "seen" by the sediments at the site.

Sequence 3 is 20 ms thick at the drill site and occurs between two unconformities (reflectors 2 and 3). Sequence 3 equates with the upper part of lithologic Unit II, defined as being composed of nannofossil-foraminifer ooze with micrite and some chalky bands, deposited in an upper bathyal environment and extending between ~75 and 90 m. The ages of these upper and lower boundaries are dated as 3.0 and 5.2 Ma. The lower boundary of sequence 3 therefore defines the boundary between the upper Miocene and Pliocene.

Sequence 4 occurs between reflectors 3 and 4 and is 50 ms thick at the drill site, occurring from 810 to 837 ms depth. It thins quickly to the east; it may be missing halfway to Site 814, but thickens substantially to the west. Sequence 4 is composed of reflectors that successively onlap to the east, climbing up the basal unconformity. Sequence 4 is equated with the lower half of lithologic Unit II, which lies between 90 and 115 mbsf and is composed of nannofossil foraminifer ooze with micrite and contains speckled dark grains and chalky bands. The lower boundary is dated at 10 Ma, the age of the middle/late Miocene boundary. This agrees well with the transgressive nature of the sequence representing the late Miocene increases in sea level following a decrease during the middle Miocene.

Sequence 5 occurs between reflectors 4 and 5, at a depth of 837 and 892 ms; it is ~50 ms thick at the drill site. Sequence 5 correlates with lithologic Unit III, defined as occurring between 115 and 160 mbsf and described as a bioclastic foraminifer ooze with micrite and nannofossils deposited in a deep neritic environment.

Sequence 6 occurs between 892 ms and the base of the hole. It equates with lithological Units IV and V, defined as dolomite micrite foraminifer chalk/ooze and dolomitized skeletal grainstone. The sediments were deposited in a shallow-water neritic environment. The foraminifer rudstone defined at a depth of 190 mbsf may relate to a strong reflector at about 900 ms in the hole.

It is remarkable how close many of the unconformities defined above follow the global cycle charts of Haq et al. (1987) for timing of major events. We advise caution, however, against overinterpretations in this direction.

Subsidence data from exploration and scientific drill holes off northeastern Australia indicate that the region has not subsided wholly as a result of uniform post-rift thermal cooling, but that subsidence pulses have occurred at different times. DSDP Site 209 suggests that the subsidence history of the Queensland Plateau has been characterized by progressively increased rates of subsidence. An initial slow rate (20

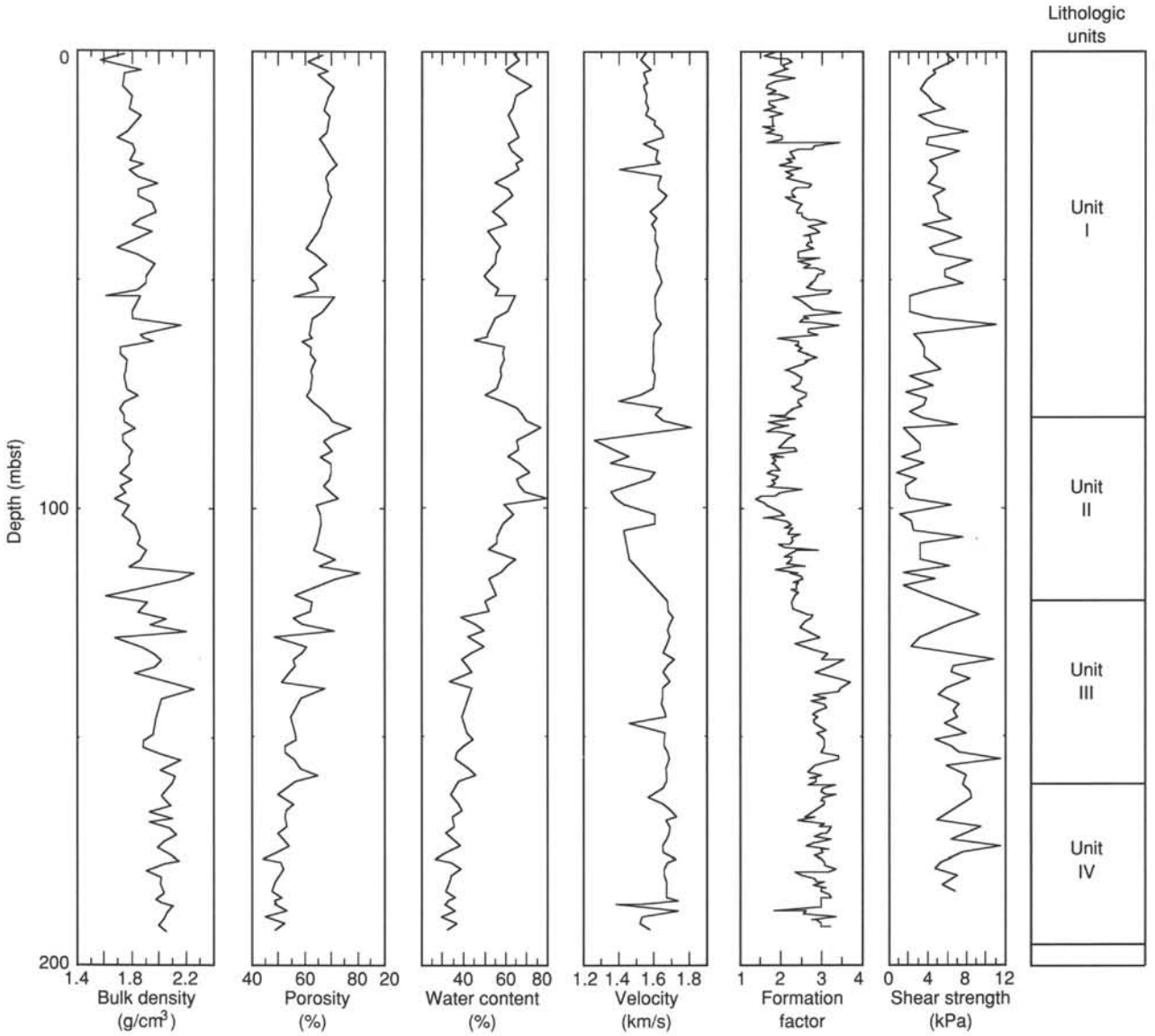


Figure 15. Summary of physical properties data from Hole 813A.

m/m.y.) was followed by an increase to 40 m/m.y. after the middle Miocene. The data from Site 811 confirms the sharply increased subsidence pulse in the early middle Miocene. The results from other drill holes will determine whether subsidence has been uniform over the plateau or whether it isdifferent in the lows and the highs. Indeed, it will be particularly interesting to compare the subsidence of northern and southern sites to test whether the plateau has tilted to the north as advocated by earlier workers (Mutter and Karner, 1980).

## REFERENCES


Andrews, J. E., 1973. Correlation of seismic reflectors. *In* Burns, R. E., Andrews, J. E., et al., *Init. Repts. DSDP,* 21: Washington (U.S. Govt. Printing Office), 459–479.

Falvey, D. A., and Mutter, J. C., 1981. Regional plate tectonics and the evolution of Australia's passive continental margins. *BMR J. Aust. Geol. Geophys.,* 6:1–29.

Feary, D. A., Pigram, C. J., Davies, P. J., Symonds, P. A., Droxler, A. W., and Peerdeman, F., 1990. Ocean Drilling Program—Leg 133 Safety package. *BMR Aust. Record,* 6.

Haq, B. U., Hardenbol, J., and Vail, P. R., 1987. Chronology of fluctuating sea levels since the Triassic. *Science,* 235:1156–1166.

Mutter, J. C., and Karner, G. D., 1980. The continental margin off northeast Australia. *In* Henderson, R. A., and Stephenson, P. J. (Eds.), *The Geology and Geophysics of Northeast Australia:* Brisbane (Geol. Soc. Aust., Queensland Div.), 47–69.

Symonds, P. A., Fritsch, J., and Scluter, J. U., 1984. Continental margin around the western Coral Sea Basin: structural elements, seismic sequences and petroleum geological aspects. *In* Watson, S. T. (Ed.), *Trans. 3rd Circum Pacific Energy Min. Res. Conf., Hawaii:* Tulsa (AAPG), 143–152.

van Morkhoven, F.P.C.M., Berggren, W. A., Edwards, A. S., et al., 1986. Cenozoic cosmopolitan deep-water benthic foraminifera. *Bull. Cent. Rech. Explor.-Prod. Elf-Aquitaine Mem.,* 11.


**Ms 133A-106**

**NOTE: All core description forms ("barrel sheets") and core photographs have been printed on coated paper and bound separately as Part 2 of this volume, beginning on page 813.**

**Table 8. Compressional wave velocity at Hole 813A.**

| Core, section, interval (cm) | Depth (mbsf) | Distance (mm) | Traveltime ($\mu$s) | Velocity (m/s) |
|---|---|---|---|---|
| 133-813A- | | | | |
| 1H-1, 10.5–10.8 | 0.10 | 27.32 | 19.70 | 1560 |
| 1H-2, 76–79 | 2.26 | 25.31 | 18.77 | 1523 |
| 1H-3, 101–104 | 4.01 | 25.61 | 18.39 | 1582 |
| 1H-4, 71–74 | 5.21 | 26.28 | 19.28 | 1536 |
| 2H-1, 121–124 | 6.91 | 26.49 | 19.16 | 1561 |
| 2H-2, 81–84 | 8.01 | 18.98 | 14.47 | 1540 |
| 2H-3, 101–104 | 9.71 | 26.93 | 19.50 | 1555 |
| 2H-4, 101–104 | 11.21 | 27.36 | 19.81 | 1552 |
| 2H-5, 66–69 | 12.36 | 26.06 | 18.80 | 1569 |
| 2H-6, 101–104 | 14.21 | 27.19 | 19.70 | 1552 |
| 2H-7, 56–59 | 15.26 | 27.10 | 19.54 | 1605 |
| 3H-1, 101–104 | 16.21 | 27.54 | 19.85 | 1601 |
| 3H-2, 101–104 | 17.71 | 27.05 | 19.13 | 1644 |
| 3H-3, 101–104 | 19.21 | 26.84 | 18.91 | 1654 |
| 3H-4, 101–104 | 20.71 | 27.58 | 20.52 | 1540 |
| 3H-5, 71–74 | 21.91 | 26.06 | 18.76 | 1618 |
| 3H-6, 101–104 | 23.71 | 26.14 | 18.89 | 1610 |
| 3H-7, 41–44 | 24.61 | 25.13 | 18.05 | 1633 |
| 4H-1, 111–114 | 25.81 | 25.92 | 20.93 | 1405 |
| 4H-2, 101–104 | 27.21 | 25.71 | 18.36 | 1638 |
| 4H-3, 111–114 | 28.81 | 27.89 | 19.84 | 1624 |
| 4H-4, 101–104 | 30.21 | 25.83 | 18.58 | 1622 |
| 4H-5, 101–104 | 31.71 | 24.98 | 17.62 | 1672 |
| 4H-6, 123–126 | 33.43 | 23.31 | 16.86 | 1640 |
| 5H-1, 101–104 | 35.21 | 26.92 | 19.72 | 1575 |
| 5H-2, 101–104 | 36.71 | 26.84 | 19.28 | 1615 |
| 5H-3, 101–104 | 38.21 | 21.29 | 16.05 | 1584 |
| 5H-4, 101–104 | 39.71 | 26.44 | 19.08 | 1609 |
| 5H-5, 101–104 | 41.21 | 25.53 | 18.54 | 1606 |
| 5H-6, 101–104 | 42.71 | 25.27 | 18.27 | 1618 |
| 6H-1, 101–104 | 44.71 | 26.70 | 19.18 | 1616 |
| 6H-2, 101–104 | 46.21 | 24.79 | 18.05 | 1609 |
| 6H-3, 101–104 | 47.71 | 26.58 | 19.14 | 1612 |
| 6H-4, 101–104 | 49.21 | 27.45 | 19.46 | 1635 |
| 6H-5, 101–104 | 50.71 | 26.41 | 18.73 | 1645 |
| 6H-6, 101–104 | 52.21 | 26.01 | 18.66 | 1626 |
| 6H-7, 52–56 | 53.22 | 27.93 | 20.02 | 1609 |
| 7H-1, 60–64 | 53.80 | 26.74 | 19.32 | 1604 |
| 7H-3, 97–100 | 57.17 | 27.37 | 19.66 | 1610 |
| 7H-4, 97–100 | 58.67 | 28.45 | 20.30 | 1613 |
| 7H-5, 97–100 | 60.17 | 28.28 | 19.96 | 1637 |
| 7H-6, 97–100 | 61.67 | 28.89 | 20.74 | 1598 |
| 7H-7, 77–81 | 62.97 | 27.54 | 19.87 | 1599 |
| 8H-1, 70–73 | 63.40 | 28.28 | 20.35 | 1598 |
| 8H-2, 70–73 | 64.90 | 28.54 | 20.53 | 1597 |
| 8H-3, 70–73 | 66.40 | 28.24 | 20.34 | 1597 |
| 8H-4, 70–73 | 67.90 | 28.41 | 20.40 | 1601 |
| 8H-5, 70–73 | 69.40 | 27.10 | 19.69 | 1590 |
| 8H-6, 70–73 | 70.90 | 26.88 | 19.40 | 1605 |
| 9H-1, 140–143 | 73.60 | 28.28 | 20.40 | 1593 |
| 9H-2, 140–143 | 75.10 | 27.14 | 20.41 | 1523 |
| 9H-3, 140–143 | 76.60 | 28.54 | 22.86 | 1400 |
| 9H-4, 140–143 | 78.10 | 24.39 | 17.52 | 1641 |
| 9H-5, 140–143 | 79.60 | 26.79 | 19.29 | 1610 |
| 9H-6, 140–143 | 81.10 | 27.45 | 19.31 | 1651 |
| 10H-1, 86–90 | 82.56 | 29.90 | 19.32 | 1808 |
| 10H-3, 86–90 | 85.56 | 29.07 | 25.28 | 1264 |
| 10H-4, 86–90 | 87.06 | 29.37 | 23.86 | 1371 |
| 10H-5, 90–93 | 88.60 | 29.71 | 22.95 | 1455 |
| 10H-6, 90–93 | 90.10 | 28.02 | 23.14 | 1352 |
| 11H-1, 90–93 | 92.10 | 28.81 | 20.59 | 1607 |
| 11H-2, 90–93 | 93.60 | 28.50 | 20.73 | 1575 |
| 11H-4, 90–93 | 96.60 | 29.37 | 24.08 | 1356 |
| 11H-5, 90–93 | 98.10 | 29.33 | 23.69 | 1381 |
| 11H-6, 90–93 | 99.60 | 28.76 | 22.66 | 1427 |
| 12H-1, 100–103 | 101.70 | 28.37 | 20.33 | 1606 |
| 12H-2, 100–103 | 103.20 | 29.02 | 20.72 | 1607 |
| 12H-3, 100–103 | 104.70 | 28.59 | 22.54 | 1427 |
| 13H-1, 100–103 | 111.20 | 29.23 | 22.54 | 1462 |
| 14H-1, 101–104 | 120.71 | 26.76 | 18.66 | 1676 |
| 14H-2, 101–104 | 122.21 | 27.19 | 18.89 | 1679 |
| 14H-3, 101–104 | 123.71 | 27.67 | 18.89 | 1711 |
| 14H-4, 101–104 | 125.21 | 28.66 | 19.67 | 1690 |
| 14H-5, 101–104 | 126.71 | 25.84 | 18.12 | 1674 |
| 14H-6, 101–104 | 128.21 | 29.41 | 20.13 | 1689 |
| 15H-1, 101–104 | 130.21 | 28.72 | 19.92 | 1668 |

**Table 8 (continued).**

| Core, section, interval (cm) | Depth (mbsf) | Distance (mm) | Traveltime ($\mu$s) | Velocity (m/s) |
|---|---|---|---|---|
| 15H-2, 101–104 | 131.71 | 28.11 | 19.70 | 1652 |
| 15H-3, 101–104 | 133.21 | 28.54 | 19.38 | 1714 |
| 15H-4, 101–104 | 134.71 | 28.01 | 19.42 | 1675 |
| 15H-5, 91–94 | 136.11 | 28.11 | 19.68 | 1654 |
| 15H-6, 101–104 | 137.71 | 27.19 | 18.77 | 1692 |
| 16H-1, 101–104 | 139.71 | 27.06 | 19.11 | 1647 |
| 16H-2, 101–104 | 141.21 | 26.80 | 18.94 | 1648 |
| 16H-3, 101–104 | 142.71 | 27.64 | 19.51 | 1642 |
| 16H-4, 101–104 | 144.21 | 27.45 | 19.24 | 1658 |
| 16H-5, 101–104 | 145.71 | 27.06 | 18.94 | 1665 |
| 16H-6, 101–104 | 147.21 | 27.19 | 21.11 | 1464 |
| 17H-1, 101–104 | 149.21 | 25.75 | 18.19 | 1660 |
| 17H-2, 101–104 | 150.71 | 25.80 | 18.26 | 1655 |
| 17H-3, 101–104 | 152.21 | 26.53 | 18.67 | 1659 |
| 17H-4, 101–104 | 153.71 | 25.53 | 17.93 | 1674 |
| 17H-5, 101–104 | 155.21 | 25.31 | 17.71 | 1685 |
| 17H-6, 101–104 | 156.71 | 24.96 | 17.66 | 1666 |
| 18H-1, 85–88 | 158.55 | 27.41 | 19.09 | 1672 |
| 18H-2, 85–88 | 160.05 | 28.68 | 19.85 | 1673 |
| 18H-3, 85–88 | 161.55 | 28.47 | 19.92 | 1652 |
| 18H-4, 85–88 | 163.05 | 28.15 | 20.61 | 1566 |
| 18H-5, 85–88 | 164.55 | 28.98 | 20.25 | 1651 |
| 18H-6, 85–88 | 166.05 | 28.36 | 19.44 | 1696 |
| 18H-7, 60–63 | 167.30 | 28.45 | 19.21 | 1727 |
| 19H-1, 80–83 | 168.00 | 28.50 | 19.81 | 1666 |
| 19H-2, 80–83 | 169.50 | 29.24 | 20.02 | 1690 |
| 19H-3, 80–83 | 171.00 | 26.67 | 18.50 | 1688 |
| 19H-4, 80–83 | 172.50 | 27.81 | 19.35 | 1670 |
| 19H-5, 80–83 | 174.00 | 26.91 | 19.01 | 1648 |
| 19H-6, 80–83 | 175.50 | 27.54 | 19.35 | 1653 |
| 19H-7, 65–68 | 176.85 | 28.63 | 19.32 | 1726 |
| 20H-1, 80–83 | 177.50 | 28.89 | 19.96 | 1675 |
| 20H-2, 80–83 | 179.00 | 28.33 | 19.81 | 1655 |
| 20H-3, 80–83 | 180.50 | 28.20 | 19.71 | 1657 |
| 20H-4, 80–83 | 182.00 | 28.41 | 19.71 | 1670 |
| 20H-5, 80–83 | 183.50 | 27.98 | 19.44 | 1671 |
| 20H-6, 80–83 | 185.00 | 28.28 | 19.62 | 1671 |
| 21H-1, 4–7 | 186.24 | 28.89 | 19.35 | 1740 |
| 20H-7, 60–62 | 186.30 | 28.84 | 21.40 | 1535 |
| 21H-2, 4–7 | 186.84 | 28.20 | 22.83 | 1384 |
| 21H-3, 30–33 | 187.94 | 29.33 | 19.61 | 1739 |
| 21H-4, 25–28 | 189.39 | 28.41 | 21.13 | 1534 |
| 21H-5, 28–31 | 190.92 | 29.28 | 21.85 | 1521 |
| 21H-6, 32–35 | 192.46 | 30.32 | 21.86 | 1578 |

**Table 9. Electrical-resistivity formation factor at Hole 813A.**

| Core, section, interval (cm) | Depth (mbsf) | Seawater (ohms) | Sample (ohms) | Formation factor |
|---|---|---|---|---|
| 133-813A- | | | | |
| 1H-1, 20 | 0.2 | 5.2 | 9.5 | 1.83 |
| 1H-1, 70 | 0.7 | 5.2 | 8.3 | 1.60 |
| 1H-1, 120 | 1.2 | 5.0 | 9.6 | 1.92 |
| 1H-2, 20 | 1.7 | 4.7 | 10.1 | 2.15 |
| 1H-2, 70 | 2.2 | 4.6 | 10.4 | 2.26 |
| 1H-2, 120 | 2.7 | 4.7 | 9.6 | 2.04 |
| 1H-3, 20 | 3.2 | 4.6 | 9.7 | 2.11 |
| 1H-3, 70 | 3.7 | 4.7 | 10.2 | 2.17 |
| 1H-3, 120 | 4.2 | 4.7 | 9.0 | 1.91 |
| 1H-4, 20 | 4.7 | 4.9 | 8.5 | 1.73 |
| 1H-4, 70 | 5.2 | 4.7 | 8.0 | 1.70 |
| 2H-1, 20 | 5.9 | 4.9 | 11.4 | 2.33 |
| 2H-1, 70 | 6.4 | 4.9 | 9.1 | 1.86 |
| 2H-1, 120 | 6.9 | 4.9 | 8.2 | 1.67 |
| 2H-2, 21 | 7.4 | 4.8 | 7.8 | 1.63 |
| 2H-2, 70 | 7.9 | 4.8 | 8.1 | 1.69 |
| 2H-2, 120 | 8.4 | 4.8 | 9.0 | 1.88 |
| 2H-3, 20 | 8.9 | 5.0 | 8.4 | 1.68 |
| 2H-3, 70 | 9.4 | 4.7 | 9.2 | 1.96 |
| 2H-3, 120 | 9.9 | 4.7 | 10.3 | 2.19 |
| 2H-4, 20 | 10.4 | 4.8 | 8.5 | 1.77 |
| 2H-4, 70 | 10.9 | 4.7 | 8.0 | 1.70 |
| 2H-4, 120 | 11.4 | 4.7 | 8.1 | 1.72 |

**Table 9 (continued).**

| Core, section, interval (cm) | Depth (mbsf) | Seawater (ohms) | Sample (ohms) | Formation factor |
|---|---|---|---|---|
| 2H-5, 20 | 11.9 | 4.7 | 8.7 | 1.85 |
| 2H-5, 70 | 12.4 | 4.7 | 7.4 | 1.57 |
| 2H-5, 120 | 12.9 | 4.7 | 8.0 | 1.70 |
| 2H-6, 20 | 13.4 | 4.8 | 9.8 | 2.04 |
| 2H-6, 70 | 13.9 | 4.7 | 8.1 | 1.72 |
| 2H-6, 120 | 14.4 | 4.6 | 8.3 | 1.80 |
| 3H-1, 20 | 15.4 | 4.7 | 8.4 | 1.79 |
| 3H-1, 70 | 15.9 | 4.7 | 8.5 | 1.81 |
| 3H-1, 120 | 16.4 | 4.7 | 7.3 | 1.55 |
| 3H-2, 20 | 16.9 | 4.9 | 9.0 | 1.84 |
| 3H-2, 70 | 17.4 | 4.9 | 8.0 | 1.63 |
| 3H-2, 120 | 17.9 | 4.9 | 8.4 | 1.71 |
| 3H-3, 20 | 18.4 | 4.9 | 9.9 | 2.02 |
| 3H-3, 70 | 18.9 | 4.9 | 9.9 | 2.02 |
| 3H-3, 120 | 19.4 | 4.9 | 8.1 | 1.65 |
| 3H-4, 20 | 19.9 | 3.3 | 11.3 | 3.42 |
| 3H-4, 70 | 20.4 | 3.2 | 9.0 | 2.81 |
| 3H-4, 120 | 20.9 | 3.2 | 8.8 | 2.75 |
| 3H-5, 20 | 21.4 | 4.0 | 9.7 | 2.43 |
| 3H-5, 70 | 21.9 | 4.0 | 8.8 | 2.20 |
| 3H-6, 20 | 22.9 | 3.9 | 9.1 | 2.33 |
| 3H-6, 70 | 23.4 | 3.9 | 8.3 | 2.13 |
| 3H-6, 120 | 23.9 | 3.9 | 8.8 | 2.26 |
| 4H-1, 20 | 24.9 | 3.9 | 7.6 | 1.95 |
| 4H-1, 70 | 25.4 | 3.9 | 9.7 | 2.49 |
| 4H-1, 120 | 25.9 | 3.8 | 8.1 | 2.13 |
| 4H-2, 20 | 26.4 | 3.8 | 8.0 | 2.11 |
| 4H-2, 70 | 26.9 | 3.8 | 8.7 | 2.29 |
| 4H-2, 120 | 27.4 | 3.8 | 8.1 | 2.13 |
| 4H-3, 20 | 27.9 | 3.8 | 9.3 | 2.45 |
| 4H-3, 70 | 28.4 | 3.8 | 9.3 | 2.45 |
| 4H-3, 120 | 28.9 | 3.3 | 9.0 | 2.73 |
| 4H-4, 20 | 29.4 | 3.3 | 8.8 | 2.67 |
| 4H-4, 70 | 29.9 | 3.8 | 9.0 | 2.37 |
| 4H-4, 120 | 30.4 | 3.8 | 8.6 | 2.26 |
| 4H-5, 20 | 30.9 | 3.8 | 8.6 | 2.26 |
| 4H-5, 70 | 31.4 | 3.8 | 8.9 | 2.34 |
| 4H-5, 120 | 31.9 | 3.7 | 7.8 | 2.11 |
| 4H-6, 20 | 32.4 | 3.7 | 8.3 | 2.24 |
| 4H-6, 70 | 32.9 | 3.7 | 9.1 | 2.46 |
| 4H-6, 120 | 33.4 | 3.2 | 8.0 | 2.50 |
| 5H-1, 20 | 34.4 | 3.1 | 7.4 | 2.39 |
| 5H-1, 70 | 34.9 | 3.1 | 7.4 | 2.39 |
| 5H-1, 120 | 35.4 | 3.2 | 8.0 | 2.50 |
| 5H-2, 20 | 35.9 | 3.1 | 7.8 | 2.52 |
| 5H-2, 70 | 36.4 | 3.1 | 8.2 | 2.65 |
| 5H-2, 120 | 36.9 | 3.1 | 8.7 | 2.81 |
| 5H-3, 20 | 37.4 | 3.1 | 9.6 | 3.10 |
| 5H-3, 70 | 37.9 | 3.1 | 8.2 | 2.65 |
| 5H-3, 120 | 38.4 | 3.1 | 8.7 | 2.81 |
| 5H-4, 20 | 38.9 | 3.1 | 8.8 | 2.84 |
| 5H-4, 70 | 39.4 | 3.1 | 9.1 | 2.94 |
| 5H-4, 120 | 39.9 | 3.2 | 8.2 | 2.56 |
| 5H-5, 20 | 40.4 | 3.2 | 8.6 | 2.69 |
| 5H-5, 70 | 40.9 | 3.2 | 8.7 | 2.72 |
| 5H-5, 120 | 41.4 | 3.3 | 9.1 | 2.76 |
| 5H-6, 20 | 41.9 | 3.3 | 8.8 | 2.67 |
| 5H-6, 70 | 42.4 | 3.3 | 8.6 | 2.61 |
| 5H-6, 120 | 42.9 | 3.3 | 9.2 | 2.79 |
| 6H-1, 20 | 43.9 | 3.2 | 7.7 | 2.41 |
| 6H-1, 70 | 44.4 | 3.2 | 7.7 | 2.41 |
| 6H-1, 120 | 44.9 | 3.2 | 7.7 | 2.41 |
| 6H-2, 20 | 45.4 | 3.2 | 9.4 | 2.94 |
| 6H-2, 70 | 45.9 | 3.2 | 7.7 | 2.41 |
| 6H-2, 120 | 46.4 | 3.1 | 8.4 | 2.71 |
| 6H-3, 20 | 46.9 | 3.1 | 7.9 | 2.55 |
| 6H-3, 70 | 47.4 | 3.1 | 8.8 | 2.84 |
| 6H-3, 120 | 47.9 | 3.2 | 9.8 | 3.06 |
| 6H-4, 20 | 48.4 | 3.2 | 9.7 | 3.03 |
| 6H-4, 70 | 48.9 | 3.2 | 9.3 | 2.91 |
| 6H-4, 120 | 49.4 | 3.3 | 9.4 | 2.85 |
| 6H-5, 20 | 49.9 | 3.4 | 9.6 | 2.82 |
| 6H-5, 70 | 50.4 | 3.3 | 8.9 | 2.70 |
| 6H-5, 120 | 50.9 | 3.2 | 8.8 | 2.75 |
| 6H-6, 20 | 51.4 | 3.3 | 8.6 | 2.61 |
| 6H-6, 70 | 51.9 | 3.3 | 9.4 | 2.85 |
| 6H-6, 120 | 52.4 | 3.2 | 10.3 | 3.22 |

**Table 9 (continued).**

| Core, section, interval (cm) | Depth (mbsf) | Seawater (ohms) | Sample (ohms) | Formation factor |
|---|---|---|---|---|
| 6H-7, 20 | 52.9 | 3.3 | 10.4 | 3.15 |
| 6H-7, 70 | 53.4 | 3.6 | 8.8 | 2.44 |
| 7H-1, 40 | 53.6 | 3.4 | 7.8 | 2.29 |
| 7H-1, 118 | 54.4 | 3.6 | 8.9 | 2.47 |
| 7H-3, 20 | 56.4 | 3.0 | 8.3 | 2.77 |
| 7H-3, 70 | 56.9 | 3.0 | 10.4 | 3.47 |
| 7H-3, 120 | 57.4 | 3.6 | 9.2 | 2.56 |
| 7H-4, 70 | 58.4 | 3.1 | 8.3 | 2.68 |
| 7H-4, 100 | 58.7 | 3.0 | 7.6 | 2.53 |
| 7H-4, 120 | 58.9 | 3.1 | 7.6 | 2.45 |
| 7H-5, 20 | 59.4 | 3.1 | 8.4 | 2.71 |
| 7H-5, 70 | 59.9 | 3.0 | 10.2 | 3.40 |
| 7H-5, 120 | 60.4 | 3.4 | 9.2 | 2.71 |
| 7H-6, 20 | 60.9 | 3.1 | 8.3 | 2.68 |
| 7H-6, 70 | 61.4 | 3.1 | 8.2 | 2.65 |
| 7H-6, 120 | 61.9 | 3.1 | 9.0 | 2.90 |
| 8H-1, 20 | 62.9 | 3.6 | 6.9 | 1.92 |
| 8H-1, 70 | 63.4 | 3.0 | 7.3 | 2.43 |
| 8H-1, 120 | 63.9 | 3.0 | 7.2 | 2.40 |
| 8H-2, 20 | 64.4 | 3.1 | 7.3 | 2.35 |
| 8H-2, 70 | 64.9 | 3.1 | 7.8 | 2.52 |
| 8H-2, 120 | 65.4 | 3.2 | 7.7 | 2.41 |
| 8H-3, 20 | 65.9 | 3.3 | 8.8 | 2.67 |
| 8H-3, 70 | 66.4 | 3.1 | 8.1 | 2.61 |
| 8H-3, 120 | 66.9 | 3.1 | 8.9 | 2.87 |
| 8H-4, 20 | 67.4 | 3.2 | 8.3 | 2.59 |
| 8H-4, 70 | 67.9 | 3.2 | 8.5 | 2.66 |
| 8H-4, 120 | 68.4 | 3.2 | 8.2 | 2.56 |
| 8H-5, 20 | 68.9 | 3.3 | 7.7 | 2.33 |
| 8H-5, 70 | 69.4 | 3.5 | 7.4 | 2.11 |
| 8H-5, 120 | 69.9 | 3.5 | 7.6 | 2.17 |
| 8H-6, 20 | 70.4 | 3.5 | 8.2 | 2.34 |
| 8H-6, 70 | 70.9 | 3.4 | 8.4 | 2.47 |
| 8H-6, 120 | 71.4 | 3.3 | 8.3 | 2.52 |
| 9H-1, 20 | 72.4 | 3.4 | 8.4 | 2.47 |
| 9H-1, 70 | 72.9 | 3.6 | 8.4 | 2.33 |
| 9H-1, 120 | 73.4 | 3.5 | 7.9 | 2.26 |
| 9H-2, 20 | 73.9 | 3.5 | 8.3 | 2.37 |
| 9H-2, 70 | 74.4 | 3.6 | 9.4 | 2.61 |
| 9H-2, 120 | 74.9 | 3.6 | 9.4 | 2.61 |
| 9H-3, 20 | 75.4 | 3.8 | 9.9 | 2.61 |
| 9H-3, 70 | 75.9 | 3.7 | 9.1 | 2.46 |
| 9H-3, 120 | 76.4 | 3.7 | 9.0 | 2.43 |
| 9H-4, 20 | 76.9 | 3.4 | 8.2 | 2.41 |
| 9H-4, 70 | 77.4 | 3.4 | 8.5 | 2.50 |
| 9H-4, 120 | 77.9 | 3.4 | 7.6 | 2.24 |
| 9H-5, 20 | 78.4 | 3.4 | 7.8 | 2.29 |
| 9H-5, 70 | 78.9 | 3.6 | 7.9 | 2.19 |
| 9H-5, 110 | 79.3 | 3.5 | 7.4 | 2.11 |
| 9H-6, 20 | 79.9 | 3.7 | 6.4 | 1.73 |
| 9H-6, 70 | 80.4 | 3.2 | 7.5 | 2.34 |
| 9H-6, 110 | 80.8 | 3.3 | 5.6 | 1.70 |
| 9H-7, 20 | 81.4 | 3.5 | 7.2 | 2.06 |
| 10H-1, 20 | 81.9 | 3.4 | 7.4 | 2.18 |
| 10H-1, 70 | 82.4 | 3.5 | 6.4 | 1.83 |
| 10H-1, 110 | 82.8 | 3.5 | 5.8 | 1.66 |
| 10H-2, 20 | 83.4 | 3.1 | 6.0 | 1.94 |
| 10H-2, 70 | 83.9 | 3.1 | 7.3 | 2.35 |
| 10H-2, 120 | 84.4 | 3.2 | 7.0 | 2.19 |
| 10H-4, 20 | 86.4 | 3.4 | 6.6 | 1.94 |
| 10H-4, 70 | 86.9 | 3.3 | 7.7 | 2.33 |
| 10H-4, 120 | 87.4 | 3.1 | 7.4 | 2.39 |
| 10H-5, 20 | 87.9 | 3.5 | 6.1 | 1.74 |
| 10H-5, 70 | 88.4 | 3.4 | 7.0 | 2.06 |
| 10H-5, 120 | 88.9 | 3.4 | 6.1 | 1.79 |
| 10H-6, 20 | 89.4 | 3.4 | 6.4 | 1.88 |
| 10H-6, 70 | 89.9 | 3.6 | 6.4 | 1.78 |
| 10H-6, 120 | 90.4 | 3.2 | 5.9 | 1.84 |
| 11H-1, 20 | 91.4 | 3.3 | 6.5 | 1.97 |
| 11H-1, 70 | 91.9 | 3.5 | 6.2 | 1.77 |
| 11H-1, 120 | 92.4 | 3.7 | 6.2 | 1.68 |
| 11H-2, 20 | 92.9 | 3.3 | 6.4 | 1.94 |
| 11H-2, 70 | 93.4 | 3.3 | 6.1 | 1.85 |
| 11H-2, 120 | 93.9 | 4.1 | 7.3 | 1.78 |
| 11H-3, 20 | 94.4 | 3.4 | 6.3 | 1.85 |
| 11H-3, 70 | 94.9 | 3.4 | 5.9 | 1.74 |
| 11H-3, 120 | 95.4 | 3.4 | 5.7 | 1.68 |

**Table 9 (continued).**

| Core, section, interval (cm) | Depth (mbsf) | Seawater (ohms) | Sample (ohms) | Formation factor |
|---|---|---|---|---|
| 11H-4, 20 | 95.9 | 3.7 | 9.3 | 2.51 |
| 11H-4, 70 | 96.4 | 3.7 | 7.3 | 1.97 |
| 11H-4, 120 | 96.9 | 3.7 | 6.9 | 1.86 |
| 11H-5, 20 | 97.4 | 3.6 | 5.5 | 1.53 |
| 11H-5, 70 | 97.9 | 3.8 | 5.3 | 1.39 |
| 11H-5, 120 | 98.4 | 3.6 | 5.7 | 1.58 |
| 11H-6, 20 | 98.9 | 3.7 | 5.9 | 1.59 |
| 11H-6, 70 | 99.4 | 3.8 | 6.3 | 1.66 |
| 12H-1, 20 | 100.9 | 3.7 | 7.4 | 2.00 |
| 12H-1, 70 | 101.4 | 3.6 | 7.5 | 2.08 |
| 12H-1, 120 | 101.9 | 4.0 | 6.3 | 1.58 |
| 12H-2, 20 | 102.4 | 3.7 | 6.5 | 1.76 |
| 12H-2, 70 | 102.9 | 3.3 | 7.1 | 2.15 |
| 12H-2, 120 | 103.4 | 3.4 | 7.6 | 2.24 |
| 12H-3, 20 | 103.9 | 3.4 | 7.1 | 2.09 |
| 12H-3, 70 | 104.4 | 3.4 | 7.8 | 2.29 |
| 12H-3, 120 | 104.9 | 3.5 | 7.7 | 2.20 |
| 12H-4, 20 | 105.4 | 3.5 | 7.6 | 2.17 |
| 12H-4, 70 | 105.9 | 3.0 | 7.4 | 2.47 |
| 12H-4, 120 | 106.4 | 3.1 | 7.0 | 2.26 |
| 12H-5, 20 | 106.9 | 3.1 | 7.1 | 2.29 |
| 12H-5, 70 | 107.4 | 3.2 | 7.1 | 2.22 |
| 12H-5, 110 | 107.8 | 3.2 | 6.2 | 1.94 |
| 12H-6, 20 | 108.4 | 3.2 | 6.7 | 2.09 |
| 12H-6, 70 | 108.9 | 3.2 | 9.3 | 2.91 |
| 12H-6, 120 | 109.4 | 3.2 | 7.6 | 2.38 |
| 13H-1, 20 | 110.4 | 3.3 | 6.9 | 2.09 |
| 13H-1, 70 | 110.9 | 3.4 | 7.7 | 2.26 |
| 13H-1, 120 | 111.4 | 3.3 | 7.4 | 2.24 |
| 13H-2, 20 | 111.9 | 3.4 | 7.3 | 2.15 |
| 13H-2, 70 | 112.4 | 3.2 | 8.3 | 2.59 |
| 13H-2, 120 | 112.9 | 3.5 | 8.2 | 2.34 |
| 13H-3, 20 | 113.4 | 3.4 | 6.4 | 1.88 |
| 13H-3, 70 | 113.9 | 3.5 | 8.4 | 2.40 |
| 13H-3, 120 | 114.4 | 3.6 | 8.0 | 2.22 |
| 13H-4, 20 | 114.9 | 3.5 | 8.7 | 2.49 |
| 13H-4, 70 | 115.4 | 3.6 | 9.1 | 2.53 |
| 13H-4, 120 | 115.9 | 3.5 | 8.1 | 2.31 |
| 13H-5, 20 | 116.4 | 3.5 | 8.5 | 2.43 |
| 13H-5, 70 | 116.9 | 3.5 | 8.3 | 2.37 |
| 13H-5, 120 | 117.4 | 3.4 | 8.1 | 2.38 |
| 13H-6, 20 | 117.9 | 3.4 | 7.6 | 2.24 |
| 13H-6, 70 | 118.4 | 3.5 | 8.5 | 2.43 |
| 13H-6, 120 | 118.9 | 3.4 | 8.0 | 2.35 |
| 14H-1, 70 | 120.4 | 3.5 | 7.9 | 2.26 |
| 14H-2, 70 | 121.9 | 3.5 | 8.0 | 2.29 |
| 14H-3, 20 | 122.9 | 3.6 | 9.6 | 2.67 |
| 14H-3, 70 | 123.4 | 3.6 | 10.0 | 2.78 |
| 14H-3, 120 | 123.9 | 3.4 | 9.3 | 2.74 |
| 14H-4, 70 | 124.9 | 3.4 | 8.8 | 2.59 |
| 14H-5, 70 | 126.4 | 3.5 | 8.6 | 2.46 |
| 14H-6, 70 | 127.9 | 2.8 | 8.3 | 2.96 |
| 15H-1, 70 | 129.9 | 2.9 | 6.8 | 2.34 |
| 15H-2, 50 | 131.2 | 2.9 | 8.2 | 2.83 |
| 15H-2, 100 | 131.7 | 2.9 | 9.1 | 3.14 |
| 15H-3, 60 | 132.8 | 2.9 | 8.7 | 3.00 |
| 15H-3, 120 | 133.4 | 2.9 | 10.3 | 3.55 |
| 15H-4, 60 | 134.3 | 2.9 | 9.3 | 3.21 |
| 15H-4, 120 | 134.9 | 2.9 | 8.8 | 3.03 |
| 15H-5, 60 | 135.8 | 2.9 | 8.2 | 2.83 |
| 15H-6, 60 | 137.3 | 2.9 | 10.0 | 3.45 |
| 15H-6, 120 | 137.9 | 2.9 | 10.7 | 3.69 |
| 16H-1, 60 | 139.3 | 2.9 | 10.0 | 3.45 |
| 16H-1, 120 | 139.9 | 2.9 | 9.9 | 3.41 |
| 16H-2, 60 | 140.8 | 2.9 | 8.1 | 2.79 |
| 16H-2, 120 | 141.4 | 2.9 | 9.0 | 3.10 |
| 16H-3, 60 | 142.3 | 3.0 | 8.2 | 2.73 |
| 16H-3, 120 | 142.9 | 3.0 | 9.2 | 3.07 |
| 16H-4, 60 | 143.8 | 3.0 | 9.4 | 3.13 |
| 16H-4, 120 | 144.4 | 3.0 | 8.7 | 2.90 |
| 16H-5, 60 | 145.3 | 3.0 | 8.3 | 2.77 |
| 16H-5, 120 | 145.9 | 3.0 | 8.7 | 2.90 |
| 16H-6, 60 | 146.8 | 2.9 | 8.1 | 2.79 |

**Table 9 (continued).**

| Core, section, interval (cm) | Depth (mbsf) | Seawater (ohms) | Sample (ohms) | Formation factor |
|---|---|---|---|---|
| 16H-6, 120 | 147.4 | 2.9 | 8.2 | 2.83 |
| 17H-1, 70 | 148.9 | 3.0 | 9.3 | 3.10 |
| 17H-1, 130 | 149.5 | 3.0 | 8.6 | 2.87 |
| 17H-2, 60 | 150.3 | 3.0 | 9.0 | 3.00 |
| 17H-2, 120 | 150.9 | 3.0 | 9.2 | 3.07 |
| 17H-3, 70 | 151.9 | 3.0 | 9.2 | 3.07 |
| 17H-4, 70 | 153.4 | 3.0 | 8.9 | 2.97 |
| 17H-5, 20 | 154.4 | 3.0 | 10.2 | 3.40 |
| 17H-5, 70 | 154.9 | 3.0 | 10.2 | 3.40 |
| 17H-5, 120 | 155.4 | 3.0 | 9.4 | 3.13 |
| 17H-6, 70 | 156.4 | 3.0 | 8.5 | 2.83 |
| 18H-1, 20 | 157.9 | 3.1 | 8.2 | 2.65 |
| 18H-1, 70 | 158.4 | 3.0 | 9.0 | 3.00 |
| 18H-1, 120 | 158.9 | 3.0 | 8.1 | 2.70 |
| 18H-2, 20 | 159.4 | 3.3 | 9.4 | 2.85 |
| 18H-2, 70 | 159.9 | 3.3 | 9.4 | 2.85 |
| 18H-2, 120 | 160.4 | 3.3 | 8.8 | 2.67 |
| 18H-3, 20 | 160.9 | 3.1 | 10.3 | 3.32 |
| 18H-3, 70 | 161.4 | 3.1 | 9.4 | 3.03 |
| 18H-3, 120 | 161.9 | 3.1 | 9.2 | 2.97 |
| 18H-4, 20 | 162.4 | 3.1 | 9.6 | 3.10 |
| 18H-4, 70 | 162.9 | 3.1 | 10.4 | 3.35 |
| 18H-4, 120 | 163.4 | 3.1 | 9.4 | 3.03 |
| 18H-5, 20 | 163.9 | 3.1 | 9.2 | 2.97 |
| 18H-5, 70 | 164.4 | 3.1 | 9.5 | 3.06 |
| 18H-5, 120 | 164.9 | 3.1 | 9.5 | 3.06 |
| 19H-1, 20 | 167.4 | 3.4 | 8.8 | 2.59 |
| 19H-1, 70 | 167.9 | 3.2 | 9.1 | 2.84 |
| 19H-1, 120 | 168.4 | 3.4 | 8.2 | 2.41 |
| 19H-2, 20 | 168.9 | 3.2 | 9.8 | 3.06 |
| 19H-2, 70 | 169.4 | 3.2 | 9.4 | 2.94 |
| 19H-2, 120 | 169.9 | 3.2 | 10.3 | 3.22 |
| 19H-3, 20 | 170.4 | 3.3 | 10.5 | 3.18 |
| 19H-3, 70 | 170.9 | 3.3 | 10.3 | 3.12 |
| 19H-3, 120 | 171.4 | 3.4 | 10.3 | 3.03 |
| 19H-4, 20 | 171.9 | 3.4 | 9.6 | 2.82 |
| 19H-4, 70 | 172.4 | 3.2 | 10.3 | 3.22 |
| 19H-4, 120 | 172.9 | 3.3 | 9.4 | 2.85 |
| 19H-5, 20 | 173.4 | 3.3 | 9.3 | 2.82 |
| 19H-5, 70 | 173.9 | 3.4 | 8.9 | 2.62 |
| 19H-5, 120 | 174.4 | 3.0 | 9.5 | 3.17 |
| 19H-6, 20 | 174.9 | 3.0 | 8.9 | 2.97 |
| 19H-6, 70 | 175.4 | 3.0 | 9.1 | 3.03 |
| 19H-6, 120 | 175.9 | 3.4 | 9.6 | 2.82 |
| 20H-1, 20 | 176.9 | 3.1 | 9.3 | 3.00 |
| 20H-1, 70 | 177.4 | 3.1 | 9.5 | 3.06 |
| 20H-1, 120 | 177.9 | 3.2 | 9.9 | 3.09 |
| 20H-2, 20 | 178.4 | 3.1 | 9.6 | 3.10 |
| 20H-2, 70 | 178.9 | 3.1 | 10.4 | 3.35 |
| 20H-2, 120 | 179.4 | 3.1 | 9.8 | 3.16 |
| 20H-3, 20 | 179.9 | 3.8 | 8.9 | 2.34 |
| 20H-3, 70 | 180.4 | 3.7 | 9.3 | 2.51 |
| 20H-3, 120 | 180.9 | 3.2 | 9.0 | 2.81 |
| 20H-4, 20 | 181.4 | 3.2 | 9.2 | 2.88 |
| 20H-4, 70 | 181.9 | 3.4 | 10.4 | 3.06 |
| 20H-4, 120 | 182.4 | 3.4 | 9.5 | 2.79 |
| 20H-5, 20 | 182.9 | 3.1 | 9.6 | 3.10 |
| 20H-5, 70 | 183.4 | 3.1 | 9.3 | 3.00 |
| 20H-5, 120 | 183.9 | 3.1 | 9.2 | 2.97 |
| 20H-6, 20 | 184.4 | 3.2 | 10.2 | 3.19 |
| 20H-6, 70 | 184.9 | 3.2 | 10.3 | 3.22 |
| 20H-6, 120 | 185.4 | 3.3 | 9.8 | 2.97 |
| 21H-2, 20 | 187.0 | 3.4 | 10.1 | 2.97 |
| 21H-2, 70 | 187.5 | 3.4 | 9.8 | 2.88 |
| 21H-3, 22 | 187.9 | 4.0 | 7.3 | 1.83 |
| 21H-3, 70 | 188.3 | 3.8 | 9.9 | 2.61 |
| 21H-3, 120 | 188.8 | 3.8 | 9.7 | 2.55 |
| 21H-4, 20 | 189.3 | 2.9 | 9.7 | 3.34 |
| 21H-4, 70 | 189.8 | 3.2 | 8.8 | 2.75 |
| 21H-4, 120 | 190.3 | 3.4 | 9.8 | 2.88 |
| 21H-5, 20 | 190.8 | 3.2 | 9.5 | 2.97 |
| 21H-5, 70 | 191.3 | 3.3 | 9.8 | 2.97 |
| 21H-5, 120 | 191.8 | 3.3 | 10.6 | 3.21 |

**Table 10. Vane shear strength data at Hole 813A.**

| Core, section, interval (cm) | Depth (mbsf) | Torque (deg.) | Strain (deg.) | Shear strength (kPa) |
|---|---|---|---|---|
| 133-813A- | | | | |
| 1H-1, 92–93 | 0.92 | 28 | 20 | 5.9 |
| 1H-2, 92–93 | 2.42 | 31 | 14 | 6.6 |
| 1H-3, 91–92 | 3.91 | 21 | 16 | 4.5 |
| 1H-4, 61–62 | 5.11 | 22 | 17 | 4.7 |
| 2H-1, 91–92 | 6.61 | 18 | 13 | 3.8 |
| 2H-2, 91–92 | 8.11 | 15 | 13 | 3.2 |
| 2H-3, 91–92 | 9.61 | 19 | 11 | 4.0 |
| 2H-4, 91–92 | 11.11 | 21 | 15 | 4.5 |
| 2H-5, 91–92 | 12.61 | 27 | 15 | 5.7 |
| 2H-6, 91–92 | 14.11 | 14 | 11 | 3.0 |
| 3H-1, 91–92 | 16.11 | 22 | 19 | 4.7 |
| 3H-2, 91–92 | 17.61 | 38 | 21 | 8.1 |
| 3H-3, 91–92 | 19.11 | 19 | 15 | 4.0 |
| 3H-4, 91–92 | 20.61 | 18 | 19 | 3.8 |
| 3H-5, 71–72 | 21.91 | 34 | 15 | 7.2 |
| 3H-6, 91–92 | 23.61 | 20 | 17 | 4.2 |
| 4H-1, 91–92 | 25.61 | 23 | 19 | 4.9 |
| 4H-2, 91–92 | 27.11 | 23 | 17 | 4.9 |
| 4H-3, 91–92 | 28.61 | 19 | 14 | 4.0 |
| 4H-4, 91–92 | 30.11 | 27 | 14 | 5.7 |
| 4H-5, 91–92 | 31.61 | 21 | 17 | 4.5 |
| 4H-6, 91–92 | 33.11 | 23 | 13 | 4.9 |
| 5H-1, 91–92 | 35.11 | 24 | 10 | 5.1 |
| 5H-2, 91–92 | 36.61 | 30 | 18 | 6.4 |
| 5H-3, 91–92 | 38.11 | 16 | 18 | 3.4 |
| 5H-4, 91–92 | 39.61 | 27 | 16 | 5.7 |
| 5H-5, 91–92 | 41.11 | 35 | 12 | 7.4 |
| 5H-6, 91–92 | 42.61 | 20 | 11 | 4.2 |
| 6H-1, 91–92 | 44.61 | 22 | 16 | 4.7 |
| 6H-2, 91–92 | 46.11 | 40 | 12 | 8.5 |
| 6H-3, 91–92 | 47.61 | 27 | 13 | 5.7 |
| 6H-4, 91–92 | 49.11 | 27 | 11 | 5.7 |
| 6H-5, 91–92 | 50.61 | 36 | 15 | 7.6 |
| 6H-6, 86–87 | 52.06 | 21 | 13 | 4.5 |
| 6H-7, 70–71 | 53.40 | 10 | 19 | 2.1 |
| 7H-3, 93–94 | 57.13 | 10 | 14 | 2.1 |
| 7H-4, 93–94 | 58.63 | 21 | 22 | 4.5 |
| 7H-5, 93–94 | 60.13 | 52 | 24 | 11.0 |
| 7H-6, 94–95 | 61.64 | 12 | 8 | 2.5 |
| 8H-1, 93–94 | 63.63 | 15 | 21 | 3.2 |
| 8H-2, 93–94 | 65.13 | 17 | 15 | 3.6 |
| 8H-3, 93–94 | 66.63 | 17 | 21 | 3.6 |
| 8H-4, 93–94 | 68.13 | 21 | 16 | 4.5 |
| 8H-5, 93–94 | 69.63 | 25 | 18 | 5.3 |
| 8H-6, 93–94 | 71.13 | 10 | 11 | 2.1 |
| 9H-1, 93–94 | 73.13 | 21 | 16 | 4.5 |
| 9H-2, 93–94 | 74.63 | 8 | 22 | 1.7 |
| 9H-3, 93–94 | 76.13 | 18 | 24 | 3.8 |
| 9H-4, 92–93 | 77.62 | 17 | 24 | 3.6 |
| 9H-5, 93–94 | 79.13 | 10 | 19 | 2.1 |
| 9H-6, 93–94 | 80.63 | 16 | 15 | 3.4 |
| 9H-7, 56–57 | 81.76 | 33 | 19 | 7.0 |
| 10H-1, 89–90 | 82.59 | 7 | 21 | 1.5 |
| 10H-2, 89–90 | 84.09 | 10 | 13 | 2.1 |
| 10H-3, 90–91 | 85.60 | 15 | 17 | 3.2 |

**Table 10 (continued).**

| Core, section, interval (cm) | Depth (mbsf) | Torque (deg.) | Strain (deg.) | Shear strength (kPa) |
|---|---|---|---|---|
| 10H-4, 90–91 | 87.10 | 15 | 18 | 3.2 |
| 10H-5, 90–91 | 88.60 | 6 | 11 | 1.3 |
| 10H-6, 90–91 | 90.10 | 17 | 14 | 3.6 |
| 11H-1, 90–91 | 92.10 | 4 | 10 | 0.8 |
| 11H-2, 90–91 | 93.60 | 13 | 18 | 2.8 |
| 11H-3, 90–91 | 95.10 | 8 | 17 | 1.7 |
| 11H-4, 90–91 | 96.60 | 8 | 7 | 1.7 |
| 11H-5, 90–91 | 98.10 | 10 | 9 | 2.1 |
| 11H-6, 90–91 | 99.60 | 30 | 14 | 6.4 |
| 12H-1, 90–91 | 101.60 | 5 | 6 | 1.1 |
| 12H-2, 90–91 | 103.10 | 11 | 15 | 2.3 |
| 12H-3, 90–91 | 104.60 | 12 | 15 | 2.5 |
| 12H-4, 90–91 | 106.10 | 36 | 19 | 7.6 |
| 12H-5, 90–91 | 107.60 | 15 | 14 | 3.2 |
| 12H-6, 90–91 | 109.10 | 15 | 14 | 3.2 |
| 13H-1, 90–91 | 111.10 | 15 | 14 | 3.2 |
| 13H-2, 90–91 | 112.60 | 29 | 20 | 6.2 |
| 13H-3, 90–91 | 114.10 | 7 | 12 | 1.5 |
| 13H-4, 90–91 | 115.60 | 22 | 14 | 4.7 |
| 13H-5, 86–87 | 117.06 | 7 | 8 | 1.5 |
| 13H-6, 87–88 | 118.57 | 14 | 18 | 3.0 |
| 14H-3, 87–88 | 123.57 | 44 | 17 | 9.3 |
| 14H-4, 87–88 | 125.07 | 30 | 16 | 6.4 |
| 14H-6, 96–97 | 128.16 | 15 | 18 | 3.2 |
| 15H-1, 91–92 | 130.11 | 11 | 16 | 2.3 |
| 15H-2, 91–92 | 131.61 | 32 | 15 | 6.8 |
| 15H-3, 91–92 | 133.11 | 51 | 14 | 10.8 |
| 15H-4, 91–92 | 134.61 | 31 | 16 | 6.6 |
| 15H-5, 81–82 | 136.01 | 30 | 16 | 6.4 |
| 15H-6, 91–92 | 137.61 | 39 | 16 | 8.3 |
| 16H-1, 91–92 | 139.61 | 28 | 16 | 5.9 |
| 16H-2, 91–92 | 141.11 | 24 | 16 | 5.1 |
| 16H-3, 91–92 | 142.61 | 34 | 16 | 7.2 |
| 16H-4, 91–92 | 144.11 | 31 | 16 | 6.6 |
| 16H-5, 92–93 | 145.62 | 33 | 18 | 7.0 |
| 16H-6, 92–93 | 147.12 | 27 | 16 | 5.7 |
| 17H-1, 91–92 | 149.11 | 37 | 15 | 7.9 |
| 17H-2, 91–92 | 150.61 | 22 | 15 | 4.7 |
| 17H-3, 91–92 | 152.11 | 30 | 17 | 6.4 |
| 17H-4, 91–92 | 153.61 | 34 | 15 | 7.2 |
| 17H-5, 91–92 | 155.11 | 54 | 17 | 11.5 |
| 17H-6, 91–92 | 156.61 | 28 | 14 | 5.9 |
| 18H-1, 104–105 | 158.74 | 37 | 12 | 7.9 |
| 18H-2, 104–105 | 160.24 | 36 | 12 | 7.6 |
| 18H-3, 104–105 | 161.74 | 39 | 16 | 8.3 |
| 18H-4, 104–105 | 163.24 | 40 | 12 | 8.5 |
| 19H-1, 92–93 | 168.12 | 23 | 12 | 4.9 |
| 19H-2, 92–93 | 169.62 | 45 | 15 | 9.5 |
| 19H-4, 90–91 | 172.60 | 30 | 15 | 6.4 |
| 19H-5, 95–96 | 174.15 | 54 | 10 | 11.5 |
| 19H-6, 98–99 | 175.68 | 36 | 13 | 7.6 |
| 20H-1, 92–93 | 177.62 | 25 | 13 | 5.3 |
| 20H-2, 92–93 | 179.12 | 22 | 13 | 4.7 |
| 20H-3, 92–93 | 180.62 | 33 | 13 | 7.0 |
| 20H-4, 92–93 | 182.12 | 26 | 13 | 5.5 |
| 20H-5, 92–93 | 183.62 | 32 | 13 | 6.8 |

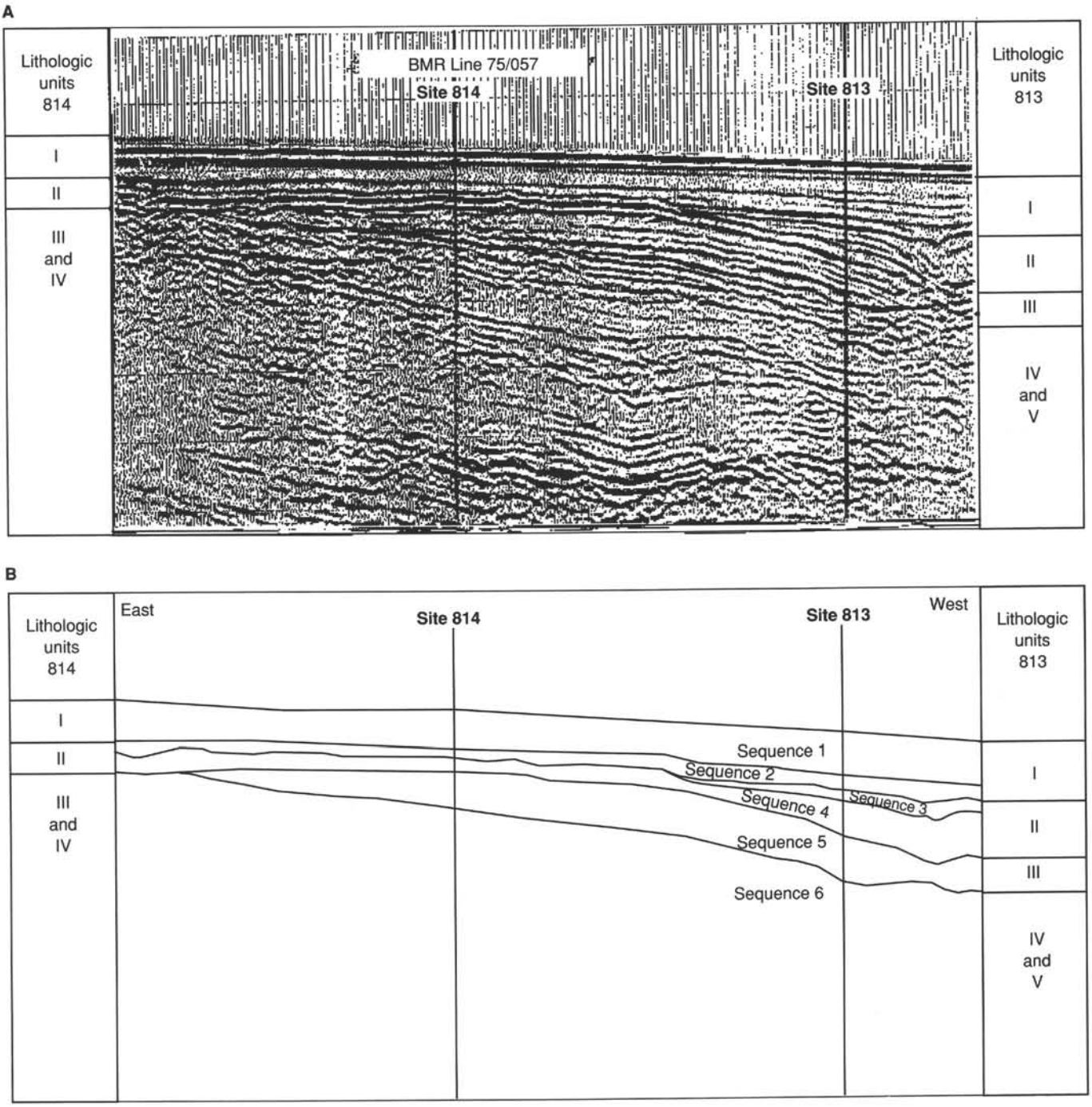


Figure 16. **A.** Seismic section connecting Sites 813 and 814. **B.** The interpreted seismic stratigraphy and lithostratigraphic correlations.